Pilot-Channel-Aided Successive Interference Cancellation for Uplink WCDMA Systems

Chih-Hsuan Tang, *Student Member, IEEE*, and Che-Ho Wei, *Fellow, IEEE*

***Abstract*—In this paper, a pilot-channel-aided successive-interference-cancellation (SIC) scheme for uplink wideband code-division multiple-access system is presented. In order to alleviate the interferences from other users' pilot-channel signals, this scheme performs pilot-channel-signal removal (PCSR) for all users before data detection. Three ordering methods for successive-cancellation process are discussed and compared in the aspect of architecture, latency, computational complexity, and error performance. In addition, channel estimation performed independently with the pilot-channel of each user is taken into consideration in the analyses. The pilot-channel-aided SIC performs variously with different ordering methods, pilot-to-traffic amplitude ratios, grouping intervals, power-distribution ratios, and propagation conditions. From our analyses and simulations, the SIC with ordering based on RAKE outputs at the first stage in properly chosen grouping interval is suggested over multipath fading channels when error performance and practicability are jointly concerned.**

***Index Terms*—Channel estimation, code-division multiple access (CDMA), ordering, pilot-channel, successive interference cancellation (SIC), third generation (3G).**

I. Introduction

DIRECT-SEQUENCE code-division multiple-access (CDMA) technique has attracted considerable attention due to its potential of high capacity and robust performance in fading channels [1], [2]. However, the capacity of CDMA systems is primarily limited by the multiple-access interference (MAI). High-power users can seriously corrupt users with low receiving power, which is known as the "near/far" problem. Therefore, much attention has been devoted to receiver schemes that are capable of canceling multiuser interference [2]. The optimal maximum-likelihood sequence estimation was first investigated in the study in [3]. To avoid the large number of computations in the optimal detector, various suboptimum detectors with lower complexity have been proposed [2], [4]–[8]. Among the suboptimum multiuser detectors, interference-cancellation (IC) techniques, including successive IC (SIC) and parallel IC (PIC) [5], [6] are considered as viable alternatives. According to a specific order, the SIC detects user data and cancels MAI in a serial manner. It has the advantage of simplicity, robustness, and having superior error performance over PIC in Rayleigh fading channels [9], [10] and nonequal user-power profile. Recent work shows SIC as a practical technique where its simplified version is employed as part of a commercial device to increase the EV-DO Rev A reverse-link voice-over-IP capacity by about 15% [11].

Several techniques have been proposed to overcome the disadvantages that prevent SIC from becoming a widely used technique [12]. First, the total decoding time increases linearly with the number of users, which can now be diminished by using a pipeline scheme [13], [14]. Second, although using SIC can reduce the other-cell interference [17], [18], and increase the system capacity [19], [20], SIC with controlled user power distribution [12], [15], [16] is somewhat complicated. Recently, a frame-error-rate-based outer loop power control is shown to be applicable to SIC [21]. In [22], a simple iterative algorithm to achieve the optimal control power distribution is given. Third, the performance of SIC is sensitive to channel-estimation accuracy due to error propagation. Pilot-channel can be employed to reduce the channel-estimation errors. In the third-generation (3G) mobile-communication systems [23], traffic- and pilot-channel signals are transmitted simultaneously by QPSK modulation. However, the traffic-channel signals are always interfered by other users' pilot and traffic signal. Pilot-channel-signal-removal technique combined with RAKE receiver [24], PIC [25], or SIC [26] can be used to alleviate the interference from other users' pilot signals.

It has been shown that the ordering method has a great effect on the error performance of SIC [28]–[31]. To determine the cancellation order, Ewerbring *et al.* [27] use the gain-ranking list obtained from channel estimates for successive cancellation. In [7], the correlator outputs pass on to a selector to find the user with the strongest correlation values for decoding and cancellation in each stage. For asynchronous systems, G bits of each user are grouped into the cancellation frame, and the ranking of the users is obtained from the averages of correlations over G bits. In [13], the average power is used to decide the cancellation order. Another method proposed is to use the signal strength obtained at the outputs of the first stage's RAKE bank as the basis for ranking detection order over multipath fading channels [26]. In [30], the effects of ordering methods on hard-decision-based SIC with equal received power over additive white Gaussian noise (AWGN) and flat Rayleigh fading channels for an asynchronous system are examined. In this paper, with a pilot-channel-signal-removed SIC in the uplink wideband code-division multiple-access (WCDMA) systems, the architectures for three ordering methods are presented for

Manuscript received August 29, 2003; revised January 4, 2005, January 19, 2006, and August 8, 2006. This work was supported in part by the National Science Council, Taiwan, R.O.C., and in part by the Lee and MTI Center for Networking Research, National Chiao Tung University. The review of this paper was coordinated by Dr. Y. Yoon.

The authors are with the Institute of Electronics, National Chiao Tung University, Hsinchu 300, Taiwan, R.O.C. (e-mail: chihhsuan.ee86g@nctu.edu.tw; chwei@mail.nctu.edu.tw).

Color versions of one or more of the figures in this paper are available online at http://ieeexplore.ieee.org.

Digital Object Identifier 10.1109/TVT.2007.897226

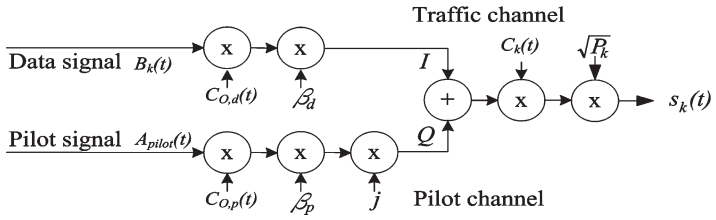

Fig. 1. Transmitter model for the kth user.

practical use. To minimize the complexity of the receiver, we adopt the maximum-ratio-combining RAKE receiver with hard decision for data detection and windowed moving average technique for channel estimation. The implementation issues, such as reordering frequency, latency, and computational complexity, are analyzed. In addition, we examine the parameters such as pilot-to-traffic amplitude ratio, ordering method, grouping interval, received-power-distribution ratio (PDR), and channel estimation, as well as timing-estimation errors. Some preliminary results with simulation over multipath fading channels are given in [31].

The rest of this paper is organized as follows. The system model is described in Section II. In Section III, the architecture of pilot-channel-aided SIC employing three ordering methods are presented and compared. SIC I decides the cancellation order according to average power as that in the study in [13]. In SIC II, the G-bit summation of the RAKE output strengths in each stage are used to find the next detected user [7]. SIC III decides the cancellation order based on the G-bit summation of the RAKE bank output strengths at the first stage. The bit-error-rate (BER) analysis considering channel-estimation errors over AWGN channel in asynchronous systems is presented in Section VI. In Section V, we examine the analytical and simulated results for the three SICs in AWGN and multipath Rayleigh fading channels. A brief conclusion is given in Section VI.

II. System Model

Consider an asynchronous CDMA system with QPSK modulation. The transmitter model for the kth user is shown in Fig. 1. The equivalent complex baseband representation of the transmitted signal at the mobile station is given by

$$s_k(t) = \sqrt{P_k}\left\{\beta_{\rm d} C_{O,d}(t) B_k(t) + j\beta_p C_{O,p} A_{\rm pilot}(t)\right\} C_k(t). \tag{1}$$

P_k is the signal power, and power distribution of all users in the system follows a PDR, where PDR $= P_k/P_{k+1} \geqq 1$ for $1 \leq k \leq K-1$ when there are K users in the system. For the sake of justice, total transmit power of all users is K with any given PDR, and $P_K = K(\text{PDR}-1)/|(\text{PDR})^K - 1|$.

β_d and β_p are the traffic- and pilot-channel gains, respectively. $\beta_d + \beta_p = 1$, and $\beta_c = \beta_p/\beta_d$ denotes the pilot-to-traffic amplitude ratio.

$B_k(t) = \Sigma b_k[n_b] p_b(t - n_b T_b)$ are the traffic-channel signals, where b_k is the binary data signal taking the values ± 1 with equal probability.

$A_{\rm pilot}(t) = \Sigma a_{\rm pilot}[n_{\rm pi}] p_{\rm pi}(t - n_{\rm pi} T_{\rm pi})$ are the uncoded pilot signals modulated at Q-channel and have the same characteristic as $B_k(t)$ but with a symbol period equal to $T_{\rm pi}$.

$C_k(t) = \Sigma(c_{k,I}[n] + c_{k,Q}[n]) p_c(t - n_c T_c)$ are the complex scramble sequences, where $\{c_{k,I}[n]\}$ and $\{c_{k,Q}[n]\}$ are the Gold sequences with period equal to the length of one frame and composed of $N(\text{SF})$ chips [23], where N is the bit number in a frame.

$C_{O,x}(t) = \Sigma c_{O,x}[n_c] p_c(t - n_c T_c)$, where $c_{O,x}$ are the orthogonal-variable-spreading-factor (OVSF) codes with period equal to SF, where SF $= T_b/T_c$ is the spreading factor for user data [23], and $\sum_{n_c} c_{O,x_1}[n_c] c_{O,x_2}[n_c] = 0$ when $x_1 \neq x_2$. In the following, $c_O = c_{O,d}$, $C_O = C_{O,d}$, and $c_{O,p}$ is neglected, since it is an all-one sequence.

p_c, p_b, and $p_{\rm pi}$ are unit power pulses with duration T_c, T_b, and $T_{\rm pi}$, respectively. $\text{SF}_{\rm pilot} = T_{\rm pi}/T_c$ is the spreading factor for pilot signal, and $F_{\rm sf} = T_{\rm pi}/T_c$.

After passing through a slowly fading channel, the received signal is represented as

$$r(t) = \sum_{k=1}^{K} \sum_{p=1}^{P} \alpha_{k,p}(t) s_k(t - \tau_{k,p}) + n(t) \tag{2}$$

where $n(t)$ is the complex AWGN with zero mean, and one-sided power spectral density $N_0 \cdot \tau_{k,p}$ and $\alpha_{k,p}(t)$ are the delay and the complex channel gain of the kth user at the pth path, respectively. $\tau_{k,p}$ are uniformly distributed random variables in $[0, T_b)$ for asynchronous systems. $\alpha_{k,p}(t)$ is still a zero-mean complex-valued Gaussian random variable without loss of generality when the carrier phase-shift part is absorbed in it [32]. For simplicity, we assume that the $\tau_{k,p}$ are perfectly estimated for all users, and the $\alpha_{k,p}(t)$ are constant in a symbol interval. $\alpha_{k,p}^{(n)} = \alpha_{k,p}(t)|_{t=\tau_{k,p}+nT_b}$, where $\sum_{p=1}^{P} E[|\alpha_{k,p}^{(n)}|^2] = 1$.

III. Pilot-Channel-Aided SIC

In this section, the pilot-channel-aided SICs with three ordering methods are presented. A group of G-bit data is detected in the sequel, i.e., the nth bit of user J is detected before or after another user's data is detected, where $mG \leq n < (m+1)G$, and m is a non-negative integer. The graphical illustration is shown in Fig. 2, where $1 \leq f \leq F$, and F is the number of RAKE fingers.

A. Channel Estimation

For ease of implementation, instead of using the optimal Wiener filter [33], a straightforward method to obtain the

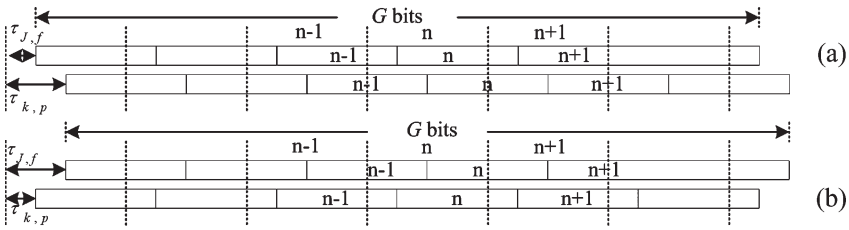

Fig. 2. Received-signal timing and data detection group (a) $\tau_{k,p;J,f} \geq 0$ and (b) $\tau_{k,p;J,f} < 0$, $\tau_{k,p;J,f} = \tau_{k,p} - \tau_{J,f}$.

channel estimate is to correlate the received signal with known pilot signal modulated at the Q-channel of user J at the fth path followed by a moving average filter to reduce the variance of the noisy channel estimates. When the channel variation is not very fast compared to WT_b, the channel estimate is

$$\hat{\alpha}^{(n)}_{\mathrm{av};J,f} = \frac{1}{W} \sum_{n_b=n-W/2}^{n+W/2-1} \left(\sqrt{P_J}\alpha^{(n_b)}_{J,f} + \mathrm{MAI}^{(n_b)}_{\hat{\alpha}_{J,f}} + I^{(n_b)}_{\hat{\alpha}_{J,f}} \right). \tag{3}$$

W is an even integer denoting the length of the moving average filter. n is assumed to be equal to or larger than $W/2$. We neglect initial channel estimates, where $n < W/2$, since the long-term system performance measurement in a real system is negligible. The scramble sequence is reused when $n + W/2 > N$.

$$\begin{aligned} \mathrm{MAI}^{(n)}_{\hat{\alpha}_{J,f}} = & a_{\mathrm{pilot}}\left[\lfloor nl \rfloor\right] \\ & \times \left[\sqrt{P_J} \sum_{p=1,p\neq f}^{P} \alpha^{(n)}_{J,p} \right. \\ & \quad \times \left\{ \frac{1}{j\beta_c} \lambda^{(n)}_{J,p;J,f}(\tau_1) + \mu^{(n)}_{J,p;J,f}(\tau_1) \right\} \\ & \quad + \sum_{k=1,k\neq J}^{K} \sqrt{P_k} \sum_{p=1}^{P} \alpha^{(n)}_{k,p} \\ & \quad \left. \times \left\{ \frac{1}{j\beta_c} \lambda^{(n)}_{k,p;J,f}(\tau) + \mu^{(n)}_{k,p;J,f}(\tau) \right\} \right] \end{aligned} \tag{4}$$

are MAI coming from other paths and other users. $l = 1/F_{\mathrm{sf}}$, and $\lfloor x \rfloor$ indicates the largest integer smaller than or equal to x. τ and τ_1 denotes $\tau_{k,p;J,f}$ and $\tau_{J,p;J,f}$, respectively.

$$I^{(n)}_{\hat{\alpha}_{J,f}} = \frac{1}{j2\beta_p T_b} \int_{nT_b+\tau_{J,f}}^{(n+1)T_b+\tau_{J,f}} A_{\mathrm{pilot}}(t-\tau_{J,f}) n(t) C^*_J(t-\tau_{J,f}) dt \tag{5}$$

is the AWGN-induced interference. $(x)^*$ denotes the complex conjugate of x. $\lambda^{(n)}_{k,p;J,f}(\tau)$ and $\mu^{(n)}_{k,p;J,f}(\tau)$ in (4) denote the interferences from other users' traffic- and pilot-channel signals, respectively, and are defined as follows:

$$\lambda^{(n)}_{k,p;J,f}(\tau) = \begin{cases} b_{\mathrm{k}}[n]\rho^{(n)}_{k,p;J,f}(\tau) + b_{\mathrm{k}}[n-1]\dot{\rho}^{(n)}_{k,p;J,f}(\tau), & \tau \geq 0 \\ b_{\mathrm{k}}[n]\rho^{(n)}_{k,p;J,f}(\tau) + b_{\mathrm{k}}[n+1]\dot{\rho}^{(n)}_{k,p;J,f}(\tau), & \tau < 0 \end{cases} \tag{6}$$

and

$$\mu^{(n)}_{k,p;J,f}(\tau) = \begin{cases} a_{\mathrm{pilot}}\left[\lfloor nl \rfloor\right] \gamma^{(n)}_{k,p;J,f}(\tau) \\ \quad + a_{\mathrm{pilot}}\left[\lfloor (n-1)l \rfloor\right] \dot{\gamma}^{(n)}_{k,p;J,f}(\tau), & \tau \geq 0 \\ a_{\mathrm{pilot}}\left[\lfloor nl \rfloor\right] \gamma^{(n)}_{k,p;J,f}(\tau) \\ \quad + a_{\mathrm{pilot}}\left[\lfloor (n+1)l \rfloor\right] \dot{\gamma}^{(n)}_{k,p;J,f}(\tau), & \tau < 0 \end{cases} \tag{7}$$

where $\rho^{(n)}_{k,p;J,f}(\tau)$, $\dot{\rho}^{(n)}_{k,p;J,f}(\tau)$, $\gamma^{(n)}_{k,p;J,f}(\tau)$, and $\dot{\gamma}^{(n)}_{k,p;J,f}(\tau)$ in (A4)–(A7) are defined in the Appendix.

B. Data Detection

After obtaining the required channel estimates, if the received signal $r(t)$ is directly sent into the correlator followed by a summation of all fingers' outputs without performing pilot-channel-signal removal, the real part of the RAKE output is given as follows:

$$\begin{aligned} \hat{Y}^{(n)}_J &= \sum_{f=1}^{F} \mathrm{Re}\left\{ \frac{1}{2\beta_d T_b} \int_{nT_b+\tau_{J,f}}^{(n+1)T_b+\tau_{J,f}} \left(\hat{\alpha}^{(n)}_{J,f}\right)^* r(t) \right. \\ & \qquad \left. \times C_O(t-\tau_{J,f}) C^*_J(t-\tau_{J,f}) dt \right\} \\ &= \sum_{f=1}^{F} \mathrm{Re}\left\{ \left(\hat{\alpha}^{(n)}_{\mathrm{av};J,f}\right)^* \left(\sqrt{P_J}\alpha^{(n)}_{J,f} b_J[n] + \mathrm{MAI}^{(n)}_{\hat{b}_{J,f}} + I^{(n)}_{\hat{b}_{J,f}} \right) \right\} \end{aligned} \tag{8}$$

where

$$\begin{aligned} \mathrm{MAI}^{(n)}_{\hat{b}_{J,f}} = & \sqrt{P_J} \sum_{p=1,p\neq f}^{P} \alpha^{(n)}_{J,p} \left\{ \lambda'^{(n)}_{J,p;J,f}(\tau_1) + j\beta_c \mu'^{(n)}_{J,p;J,f}(\tau_1) \right\} \\ & + \sum_{k=1,k\neq J}^{K} \sqrt{P_k} \sum_{p=1}^{P} \alpha^{(n)}_{k,p} \left\{ \lambda'^{(n)}_{k,p;J,f}(\tau) + j\beta_c \mu'^{(n)}_{k,p;J,f}(\tau) \right\} \end{aligned} \tag{9}$$

and

$$I^{(n)}_{\hat{b}_{J,f}} = \frac{1}{2\beta_d T_b} \int_{nT_b+\tau_{J,f}}^{(n+1)T_b+\tau_{J,f}} n(t) C_O(t-\tau_{J,f}) C^*_J(t-\tau_{J,f}) dt. \tag{10}$$

$\lambda'^{(n)}_{k,p;J,f}$ and $\mu'^{(n)}_{J,p;J,f}$ have the same definition as $\lambda^{(n)}_{k,p;J,f}(\tau)$ in (6) and $\mu^{(n)}_{k,p;J,f}(\tau)$ in (7), respectively, except that $\rho^{(n)}_{k,p;J,f}(\tau)$, $\dot{\rho}^{(n)}_{k,p;J,f}(\tau)$, $\gamma^{(n)}_{k,p;J,f}(\tau)$, and $\dot{\gamma}^{(n)}_{k,p;J,f}(\tau)$ are replaced by $\rho'^{(n)}_{k,p;J,f}(\tau)$, $\dot{\rho}'^{(n)}_{k,p;J,f}(\tau)$, $\gamma'^{(n)}_{k,p;J,f}(\tau)$, and $\dot{\gamma}'^{(n)}_{k,p;J,f}(\tau)$, respectively [defined in (A8)–(A11) in the Appendix]. It is shown in (9) that the second and the fourth interference terms come from the pilot-channel signal of multipath and other users, respectively. To remove these MAIs, $r(t)$ in (8) is replaced by $\hat{\tilde{r}}(t) = r(t) - \sum_{k=1}^{K} \hat{C}_{\text{pilot};k}(t)$, where the estimated pilot signal of user k is

$$\hat{C}_{\text{pilot};k}(t) = \sum_{p=1}^{F} j\beta_p \hat{\alpha}^{(\lfloor t-\tau_{k,p}/T_b \rfloor)}_{\text{av};k,p} \times a_{\text{pilot}}\left[\lfloor l(t-\tau_{k,p})/T_b \rfloor\right] C_k(t-\tau_{k,p}). \quad (11)$$

$\hat{Y}^{(n)}_J$, $\text{MAI}^{(n)}_{\hat{b}J,f}$, and $I^{(n)}_{\hat{b}J,f}$ in (8) become $\hat{\tilde{Y}}^{(n)}_J$, $\text{MAI}^{(n)}_{\hat{\tilde{b}}\ J,f}$, and $I^{(n)}_{\hat{\tilde{b}}\ J,f}$, respectively, where

$$\begin{aligned}\text{MAI}^{(n)}_{\hat{\tilde{b}}\ J,f} &= \sqrt{P_J} \sum_{p=1,p\neq f}^{P} \alpha^{(n)}_{J,p} \lambda'^{(n)}_{J,p;J,f}(\tau_1) \\ &\quad + \sum_{k=1,k\neq J}^{K} \sqrt{P_k} \sum_{p=1}^{P} \alpha^{(n)}_{k,p} \lambda'^{(n)}_{k,p;J,f}(\tau) \\ &\quad + j\beta_c \Bigg\{ \sqrt{P_J} \sum_{p=F+1}^{P} \alpha^{(n)}_{J,p} \mu'^{(n)}_{J,p;J,f}(\tau_1) \\ &\qquad + \sum_{k=1,k\neq J}^{K} \sqrt{P_k} \sum_{p=F+1}^{P} \alpha^{(n)}_{k,p} \mu'^{(n)}_{k,p;J,f}(\tau) \Bigg\} \\ &\quad - j\beta_c \Bigg\{ \sum_{p=1,p\neq f}^{F} \hat{\sigma}'^{(n)}_{J,p;J,f}(\tau_1) \\ &\qquad + \sum_{k=1,k\neq J}^{K} \sum_{p=1}^{F} \hat{\sigma}'^{(n)}_{k,p;J,f}(\tau) \Bigg\} \end{aligned} \quad (12)$$

with

$$\hat{\sigma}'^{(n)}_{k,p;J,f}(\tau) = \begin{cases} a_{\text{pilot}}\left[\lfloor nl \rfloor\right] \text{MAI}^{(n)}_{\hat{\alpha}_{\text{av};k,p}} \gamma'^{(n)}_{k,p;J,f}(\tau) \\ \quad + a_{\text{pilot}}\left[\lfloor (n-1)l \rfloor\right] \text{MAI}^{(n-1)}_{\hat{\alpha}_{\text{av};k,p}} \dot{\gamma}'^{(n)}_{k,p;J,f}(\tau), & \tau \geq 0 \\ a_{\text{pilot}}\left[\lfloor nl \rfloor\right] \text{MAI}^{(n)}_{\hat{\alpha}_{\text{av};k,p}} \gamma'^{(n)}_{k,p;J,f}(\tau) \\ \quad + a_{\text{pilot}}\left[\lfloor (n+1)l \rfloor\right] \text{MAI}^{(n+1)}_{\hat{\alpha}_{\text{av};k,p}} \dot{\gamma}'^{(n)}_{k,p;J,f}(\tau), & \tau < 0. \end{cases} \quad (13)$$

The AWGN-induced interference $I^{(n)}_{\hat{\tilde{b}}\ J,f}$ is expressed as

$$I^{(n)}_{\hat{\tilde{b}}\ J,f} = I^{(n)}_{\hat{b}_{J,f}} - j\beta_c \times \left(\sum_{k=1,k\neq J}^{K} \sum_{p=1}^{F} \dot{\varsigma}'^{(n)}_{k,p;J,f}(\tau) + \sum_{p=1,p\neq f}^{F} \dot{\varsigma}'^{(n)}_{J,p;J,f}(\tau_1) \right) \quad (14)$$

where

$$\hat{\varsigma}'^{(n)}_{k,p;J,f}(\tau) = \begin{cases} I^{(n)}_{\hat{\alpha}_{\text{av};k,p}} \alpha_{\text{pilot}}\left[\lfloor nl \rfloor\right] \gamma'^{(n)}_{k,p;J,f}(\tau) \\ \quad + I^{(n-1)}_{\hat{\alpha}_{\text{av};k,p}} \alpha_{\text{pilot}}\left[\lfloor (n-1)l \rfloor\right] \dot{\gamma}'^{(n)}_{k,p;J,f}(\tau), & \tau \geq 0 \\ I^{(n)}_{\hat{\alpha}_{\text{av};k,p}} \alpha_{\text{pilot}}\left[\lfloor nl \rfloor\right] \gamma'^{(n)}_{k,p;J,f}(\tau) \\ \quad + I^{(n+1)}_{\hat{\alpha}_{\text{av};k,p}} \alpha_{\text{pilot}}\left[\lfloor (n+1)l \rfloor\right] \dot{\gamma}'^{(n)}_{k,p;J,f}(\tau), & \tau < 0. \end{cases} \quad (15)$$

Both $\hat{\sigma}'^{(n)}_{k,p;J,f}(\tau)$ and $\hat{\varsigma}'^{(n)}_{k,p;J,f}(\tau)$ in (13) and (15) come from the channel-estimation errors.

In the following, SIC is performed to alleviate the MAI from other users. Generally speaking, signals are detected and canceled in order of their strength since the user with large received-signal power is more reliable but leads to serious interference to other users. However, as shown in (8), the transmitted-signal power P, channel gain α, and correlation terms, such as λ' and μ', all affect the received-signal strength and MAI to other users. Three ordering methods based on different consideration are described as follows.

1) SIC I—Ordering Based on Average Power: In SIC I, the cancellation order is decided by the average power measured over a period much longer than $1/f_d$, where f_d is the Doppler shift. According to computer simulations, $f_d/12$ is large enough to be used as the reordering frequency. When the stationary channel is assumed, the reordering frequency can be much less than $f_d/12$. To detect a group of G-bit data of all users, the architecture for SIC I is shown in Fig. 3, where the index in $\{\cdot\}$ at the output of each block denotes the processing step, and $\langle u \rangle_n = J$ denotes that the user with index J at bit index n is detected in the uth order/stage. For notational simplicity, n is omitted in the following. After performing channel estimation {1} and pilot-channel signal removing {2}, all information in Buffer A are sent to Buffer B in each G-bit interval {3}, and Buffer A can continue to collect the next G-bit information without delay. At this moment, through the buslike connection (bold line in part II), the user index and the corresponding channel estimates of the first detected user are sent to RAKE {4} followed by Decision {5}. Then, data respreading {6} and traffic-channel signal removing {7} are performed, and the remaining signal is sent back to Buffer B {8}. $\hat{\tilde{r}}_{\text{SIC};u}(t) = \hat{\tilde{r}}(t)$ when $u = 1$. After that, according to the cancellation order decided in part I, steps $5u-1$ to $5u+3$ are repeated for all the other users, where $2 \leq u \leq K$.

2) SIC II—Ordering Based on RAKE Outputs After G-Bit Cancellation of One User: In SIC II, the G-bit summation of the RAKE output strengths in each stage are used to find the next detected user. The architecture of SIC II is shown in Fig. 4. At first, we find the user with the maximum $\sum_{n=mG}^{(m+1)G-1} |\hat{\tilde{Y}}'^{(n)}_{\text{SIC}k}|$ at the output of RAKE bank in part II {5} with the Finding Max block, and sent the user index to Buffer B {6}, where $\hat{\tilde{Y}}'^{(n)}_{\text{SIC}k} = \hat{\tilde{Y}}^{(n)}_k$ and $\hat{\tilde{Y}}^{(n)}_{\text{SIC}\langle u \rangle} = \hat{\tilde{Y}}^{(n)}_J$ with $u = 1$. With this index, decision making {7}, data respreading {8}, and removing from $\hat{\tilde{r}}(t)$ {9} are performed followed by storing the remaining signal $\hat{\tilde{r}}_{\text{SIC};u+1}(t)$ in Buffer B. Then, u is increased by one, and steps $6u-2$ to $6u+3$ are repeated,

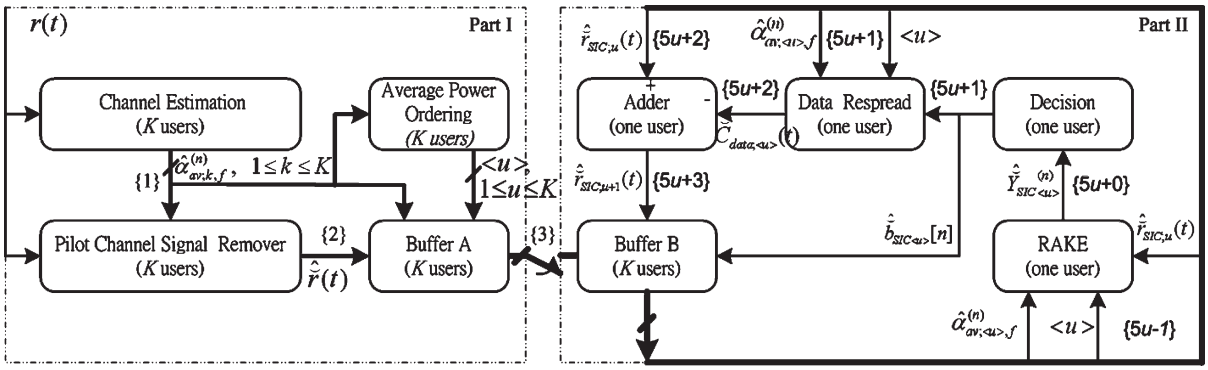

Fig. 3. Block diagram of SIC I with PCSR $(1 \le f \le F)$.

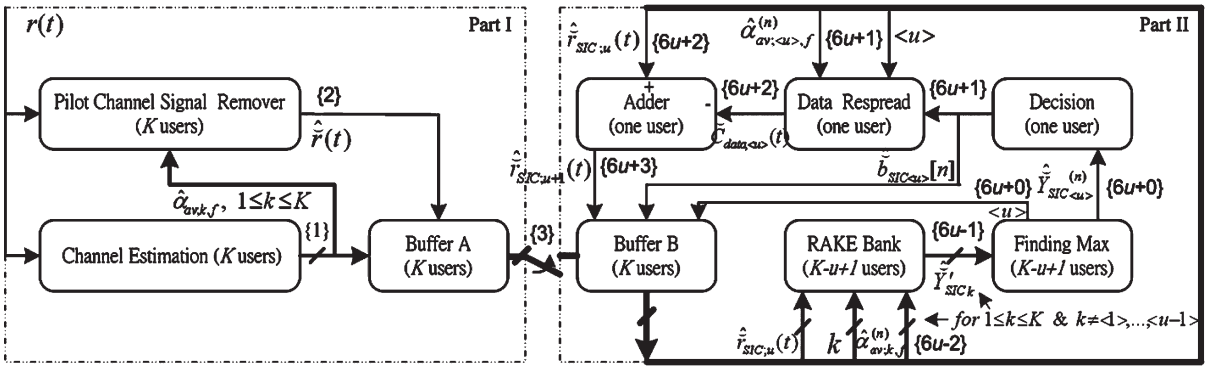

Fig. 4. Block diagram of SIC II with PCSR $(1 \le f \le F)$.

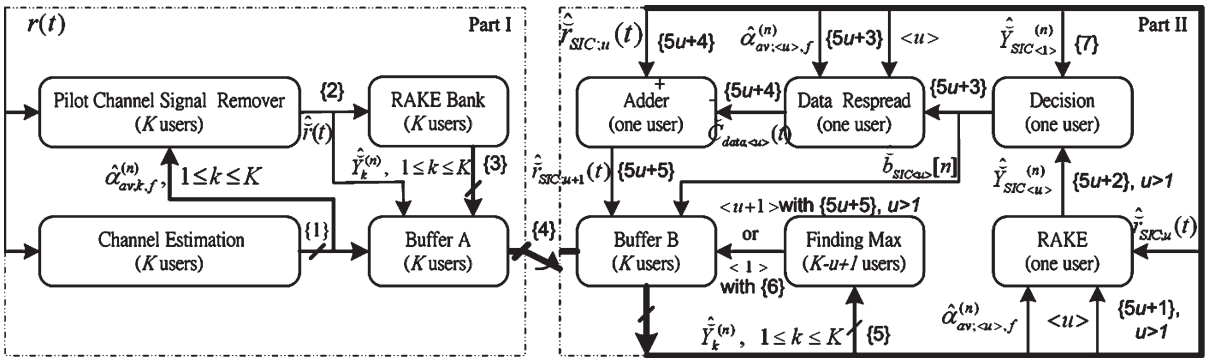

Fig. 5. Block diagram of SIC III with PCSR $(1 \le f \le F)$.

where $2 \le u \le K$. $\hat{\tilde{Y}}'^{(n)}_{\mathrm{SIC}k}$ can be obtained from (8), where J, $\hat{Y}^{(n)}_J$, and $\hat{\tilde{r}}(t)$ in (8) are replaced by k, $\hat{\tilde{Y}}'^{(n)}_{\mathrm{SIC}k}$, and $\hat{\tilde{r}}_{\mathrm{SIC};u}(t)$, respectively. Note that the Finding Max block must suspend and wait until $\hat{\tilde{Y}}'^{(n)}_{\mathrm{SIC}k}$ are shown at the outputs of RAKE bank, where k denotes all the undetected users.

3) SIC III—Ordering Based on RAKE Outputs at First Stage in Each G-Bit Interval: In SIC III, the cancellation order is decided according to the signal strength of $\sum_{n=mG}^{(m+1)G-1} |\hat{\tilde{Y}}^{(n)}_k|$ obtained in RAKE bank in part I {3}, as shown in Fig. 5. In each G-bit interval, information of all users are sent to Buffer B {4}. Then, in Finding Max block, the index of the user with maximum $\sum_{n=mG}^{(m+1)G-1} |\hat{\tilde{Y}}^{(n)}_k|$ is found {6} and then sent back to Buffer B. When the first user $(u = 1)$ is detected {8}, respread {9}, and canceled from $\hat{\tilde{r}}(t)$ {10}, the Finding Max block finds the user with the second largest signal strength according to the same $\sum_{n=mG}^{(m+1)G-1} |\hat{\tilde{Y}}^{(n)}_k|$ at the same time {10}. Thus, the RAKE output of the second detected user can be obtained right after $\hat{\tilde{r}}_{\mathrm{SIC};2}(t)$ is sent out of Buffer B. For $2 \le u \le K$, steps $5u + 1$ to $5u + 5$ are repeated.

For all SICs, in order to remove interferences from the pilot-channel signals of all users in the nth bit interval where $mG \le n < (m + 1)G$, $\hat{\tilde{r}}(t)$ with $t > [(m + 1)G + 1]T_b$ in Buffer A are sent to Buffer B. After G-bit data of all users are detected, the remaining signal $\hat{\tilde{r}}_{\mathrm{SIC};K+1}(t)$ with $t \ge (m + 1)GT_b$ are cascaded with the incoming $\hat{\tilde{r}}(t)$ for the next G-bit data detection. Ordering in SIC I only takes the transmitted power and long-term channel gain into consideration. This ordering method is often used in literature when SIC is compared with other ICs. SIC II and SIC III take advantages of instant

TABLE I
CHARACTERISTICS OF THREE SICS PER G BITS PER K USERS

SIC	I	II	III
Reordering Frequency (denoted as *RF*)	$<<f_d$	$K/(GT_b)$	$1/(GT_b)$
Throughput (Bits/Step)	$G/5$	$G/6$	$G/5$
Latency (Steps)	$5K+3$	$6K+3$	$5K+5$
Hardware Required for Minimum Delay	As shown in block diagrams in Fig. 3 ~ Fig. 5		
Computational Complexity C(.) BASE=PCSR+CE +DS+RAKE+DR+AD	$K*C$(BASE) $+K*C$(OR)* $GfdTb/RF$	$K*C$(BASE) $+K*C$(FM) $+K(K\text{-}1)/2$* C(RAKE)	$K*C$(BASE) $+K*C$(FM) $+(K\text{-}1)$* C(RAKE)

PCSR: Pilot Channel Signal Removal; CE: Channel Estimation; DS: Decision; DR: Data Respread; AD: Adder; FM: Find Max; OR: Average Power

received-signal strength, i.e., ordering is based on the compromise between reliability and channel estimates (weighting of the MAI), where SIC III is the simplified version of SIC II. Grouping interval G is used to decrease MAI due to asynchronous reception. Increasing grouping interval G can decrease uncanceled MAI to late detected users due to asynchronous reception. However, there is tradeoff between alleviating extra MAI and sensitivity to instant signal strength in SIC II and SIC III. For these two SICs, the early detected users may have small instantaneous SNR within a bit interval, as G increases.

In Table I, the reordering frequency, throughput, latency, and computational complexity of three SICs are summarized. The processes in part I of all SICs can be pipelined, since they do not need feedback information from part II.

For all SICs at nth bit interval, the real part of RAKE output in (8) of the uth canceled user with input $\hat{\breve{r}}_{\mathrm{SIC};u}(t)$ is

$$\begin{aligned}\hat{\breve{Y}}^{(n)}_{\mathrm{SIC}_{\langle u\rangle}} &= P_{\langle u\rangle}\sum_{f=1}^{F}\left|\alpha^{(n)}_{\langle u\rangle}\right|^2 b_{\langle u\rangle}[n] \\ &\quad+\sum_{f=1}^{F}\mathrm{Re}\left\{\sqrt{P_{\langle u\rangle}}\left(\alpha^{(n)}_{\langle u\rangle,f}\right)^*\right. \\ &\qquad\left.\times\left(\mathrm{MAI}^{(n)}_{\hat{\breve{b}}\,\mathrm{SIC}_{\langle u\rangle,f}}+I^{(n)}_{\hat{\breve{b}}\,\mathrm{SIC}_{\langle u\rangle,f}}\right)\right\} \\ &\quad+\left\{\left(\mathrm{MAI}^{(n)}_{\hat{\alpha}_{\mathrm{av};\langle u\rangle,f}}+I^{(n)}_{\hat{\alpha}_{\mathrm{av};\langle u\rangle,f}}\right)^*\right. \\ &\qquad\times\left(\sqrt{P_{\langle u\rangle}}\alpha^{(n)}_{\langle u\rangle,f}b_{\langle u\rangle}[n]\right. \\ &\qquad\left.\left.+\mathrm{MAI}^{(n)}_{\hat{\breve{b}}\,\mathrm{SIC}_{\langle u\rangle,f}}+I^{(n)}_{\hat{\breve{b}}\,\mathrm{SIC}_{\langle u\rangle,f}}\right)\right\} \qquad (16)\end{aligned}$$

where $\hat{\breve{r}}_{\mathrm{SIC};u}(t)=\hat{\breve{r}}(t)-\sum_{k=\langle 1\rangle}^{\langle u-1\rangle}\breve{C}_{\mathrm{data},k}(t)$, and

$$\begin{aligned}\breve{C}_{\mathrm{data};k}(t)&=\sum_{p=1}^{F}\beta_d\hat{\alpha}^{(\lfloor t-\tau_{k,p}/T_b\rfloor)}_{\mathrm{av};k,p}\hat{\breve{b}}_{\mathrm{SIC};k}\left[\lfloor(t-\tau_{k,p})/T_b\rfloor\right] \\ &\quad\times C_O(t-\tau_{k,p})C_k(t-\tau_{k,p}). \qquad (17)\end{aligned}$$

$mGT_b\le t-\tau_{k,p}<(m+1)GT_b$. $\hat{\breve{b}}_{\mathrm{SIC};k}[n]$ is the data decision where $\hat{\breve{b}}_{\mathrm{SIC};k}[n]=\mathrm{sgn}\{\hat{\breve{Y}}^{(n)}_{\mathrm{SIC}k}\}$ for $\langle 1\rangle <= k <= \langle u-1\rangle$. It is shown in (18), shown at the bottom of the page,

$$\begin{aligned}\mathrm{MAI}^{(n)}_{\hat{\breve{b}}\,\mathrm{SIC}_{\langle u\rangle,f}} &= \underbrace{j\beta_c\left\{\sqrt{P_J}\sum_{p=F+1}^{P}\alpha^{(n)}_{\langle u\rangle,p}\mu'^{(n)}_{\langle u\rangle,p;\langle u\rangle,f}(\tau_1)+\sum_{k=1,k\neq J}^{K}\sqrt{P_k}\sum_{p=F+1}^{P}\alpha^{(n)}_{k,p}\mu'^{(n)}_{k,p;\langle u\rangle,f}(\tau)\right\}}_{\text{from uncanceled pilot}} \\ &\quad+\underbrace{\sqrt{P_{\langle u\rangle}}\sum_{p=1,p\neq f}^{P}\alpha^{(n)}_{\langle u\rangle,p}\lambda'^{(n)}_{\langle u\rangle,p;\langle u\rangle,f}(\tau_1)}_{\text{from uncanceled multipath}}+\underbrace{\sum_{k=\langle u+1\rangle}^{\langle K\rangle}\sqrt{P_k}\sum_{p=1}^{P}\alpha^{(n)}_{k,p}\lambda'^{(n)}_{k,p;\langle u\rangle,f}(\tau)}_{\text{from uncanceled user}} \\ &\quad+\underbrace{\sum_{k=\langle 1\rangle}^{\langle u-1\rangle}\sqrt{P_k}\sum_{p=F+1}^{P}\alpha^{(n)}_{k,p}\lambda'^{(n)}_{k,p;\langle u\rangle,f}(\tau)}_{\text{from uncanceled multipath of canceled users}} \\ &\quad-\underbrace{j\beta_c\left\{\sum_{p=1,p\neq f}^{F}\hat{\sigma}'^{(n)}_{\langle u\rangle,p;\langle u\rangle,f}(\tau_1)+\sum_{k=1,k\neq J}^{K}\sum_{p=1}^{F}\hat{\sigma}'^{(n)}_{k,p;\langle u\rangle,f}(\tau)\right\}}_{\text{from imperfect pilot removal}} \\ &\quad-\underbrace{\left\{\sum_{p=1,p\neq f}^{F}\hat{\breve{\varphi}}'^{(n)}_{\mathrm{SIC};\langle u\rangle,p;\langle u\rangle,f}(\tau_1)+\sum_{k=\langle 1\rangle}^{\langle u-1\rangle}\sum_{p=1}^{F}\hat{\breve{\varphi}}'^{(n)}_{\mathrm{SIC};k,p;\langle u\rangle,f}(\tau)\right\}}_{\text{from imperfect channel estimation \& incorrect data decision}} \qquad (18)\end{aligned}$$

where τ denotes $\tau_{k,p;\langle u\rangle,f}$, and τ_1 denotes $\tau_{\langle u\rangle,p;\langle u\rangle,f}$. In (18)

$$\lambda'^{(n)}_{k,p;\langle u\rangle,f}(\tau) = \left\{ \begin{array}{ll} b_{\rm k}[n]\rho'^{(n)}_{k,p;\langle u\rangle,f}(\tau), & n=mG \\ b_{\rm k}[n]\rho'^{(n)}_{k,p;\langle u\rangle,f}(\tau) & \\ \quad + b_{\rm k}[n-1]\dot{\rho}'^{(n)}_{k,p;\langle u\rangle,f}(\tau), & \text{otherwise} \\ b_{\rm k}[n]\rho'^{(n)}_{k,p;\langle u\rangle,f}(\tau) + b_{\rm k}[n+1]\dot{\rho}'^{(n)}_{k,p;\langle u\rangle,f}(\tau), & \tau<0 \end{array} \right\}, \quad \tau \geq 0 \tag{19}$$

and (20), shown at the bottom of the page, with $\Delta_k^{(n)}=1$ when $b_k[n] \neq \hat{\breve{b}}_{{\rm SIC};k}[n]$, and $\Delta_k^{(n)}=0$ when $b_k[n]=\hat{\breve{b}}_{{\rm SIC};k}[n]$. The noise related interference is as follows:

$$I^{(n)}_{\hat{\breve{b}}_{{\rm SIC}\langle u\rangle,f}} = I^{(n)}_{\hat{\breve{b}}_{\langle u\rangle,f}} - \left\{ \sum_{p=1,p\neq f}^{F} \hat{\breve{\psi}}'^{(n)}_{{\rm SIC};\langle u\rangle,p;\langle u\rangle,f}(\tau_1) + \sum_{k=\langle 1\rangle}^{\langle u-1\rangle} \sum_{p=1}^{F} \hat{\breve{\psi}}'^{(n)}_{{\rm SIC};k,p;\langle u\rangle,f}(\tau) \right\} \tag{21}$$

where we have (22), shown at the bottom of the page. $\Omega_k^{(n)}=1$ when $b_k[n] \neq \hat{\breve{b}}_{{\rm SIC};k}[n]$, and $\Omega_k^{(n)}=-1$ when $b_k[n]=\hat{\breve{b}}_{{\rm SIC};k}[n]$. The detection error is denoted as $\varepsilon^{(n)}_{r\hat{b}{\rm SIC};\langle u\rangle} = 2\Delta^{(n)}_{\langle u\rangle} b_{\langle u\rangle}[n]$.

IV. Performance Analysis in AWGN Channel

In this section, a closed-form expression for the average BER in AWGN channel is presented. The pilot-channel-aided SICs employing three ordering methods accompany with channel estimation are analyzed in asynchronous systems (but assumed chip synchronous, i.e., $\tau \neq 0$ and $\tau' \neq 0$, where τ and τ' are defined in the Appendix).

A. Channel Estimation

For the sake of simplicity, the long scramble sequences are viewed as random sequences, where c_s are modeled as independent identically distributed random variables. The code correlations are assumed to be zero-mean complex-valued Gaussian random variables, where $\mathrm{Var}(\mathrm{Re}[\lambda^{(n)}_{k;J}(\tau_{k,J})]) = \mathrm{Var}(\mathrm{Re}[\mu^{(n)}_{k;J}(\tau_{k,J})]) = 1/(2\mathrm{SF})$ when chip synchronous assumption is made, and when chip asynchronous assumption is made, $\mathrm{Var}(\mathrm{Re}[\lambda^{(n)}_{k;J}(\tau_{k,J})]) = \mathrm{Var}(\mathrm{Re}[\mu^{(n)}_{k;J}(\tau_{k,J})]) = 1/(3\mathrm{SF})$ [13]. $I^{(n)}_{\hat{\alpha}J}$ is also a zero-mean complex-valued Gaussian random variable. It can be shown that the mean-squared error (MSE) of the channel estimates is given by

$$\mathrm{MSE}\left(\hat{\alpha}^{(n)}_{{\rm av};J}\right) = \frac{1}{W} E\left[\left|\hat{\alpha}^{(n)}_J - \sqrt{P_J}\alpha^{(n)}_J\right|^2\right] = \frac{1}{W}\left(\frac{\beta_c^2+1}{\beta_c^2}\right)\left(\sum_{k=1;k\neq J}^{K}\frac{P_K}{(\mathrm{SF})}+\frac{N_0}{2T_b}\right). \tag{23}$$

B. Data Detection

Without loss of generality, the time dependence is negligible in the following discussions. Thus, from (18), the decision

$$\hat{\breve{\varphi}}'^{(n)}_{{\rm SIC};k;\langle u\rangle}(\tau) = \left\{ \begin{array}{ll} \left\{{\rm MAI}^{(n)}_{\hat{\alpha}_{{\rm av};k,p}} - 2\left(\sqrt{p_k}\alpha^{(n)}_{k,p} + {\rm MAI}^{(n)}_{\hat{\alpha}_{{\rm av};k,p}}\right)\Delta^{(n)}_k\right\} b_{\rm k}[n]\rho'^{(n)}_{k,p;\langle u\rangle,f}(\tau) & \\ \quad + \left\{{\rm MAI}^{(n-1)}_{\hat{\alpha}_{{\rm av};k,p}} - 2\left(\sqrt{p_k}\alpha^{(n-1)}_{k,p} + {\rm MAI}^{(n-1)}_{\hat{\alpha}_{{\rm av};k,p}}\right)\Delta^{(n-1)}_k\right\} b_{\rm k}[n-1]\dot{\rho}'^{(n)}_{k,p;\langle u\rangle,f}(\tau) & \tau\geq 0 \\ \left\{{\rm MAI}^{(n)}_{\hat{\alpha}_{{\rm av};k,p}} - 2\left(\sqrt{p_k}\alpha^{(n)}_{k,p} + {\rm MAI}^{(n)}_{\hat{\alpha}_{{\rm av};k,p}}\right)\Delta^{(n)}_k\right\} b_{\rm k}[n]\rho'^{(n)}_{k,p;\langle u\rangle,f}(\tau) & \\ \quad + b_{\rm k}[n+1]\dot{\rho}'^{(n)}_{k,p;\langle u\rangle,f}(\tau), & n=(m+1)G-1 \\ \left\{{\rm MAI}^{(n)}_{\hat{\alpha}_{{\rm av};k,p}} - 2\left(\sqrt{p_k}\alpha^{(n)}_{k,p} + {\rm MAI}^{(n)}_{\hat{\alpha}_{{\rm av};k,p}}\right)\Delta^{(n)}_k\right\} b_{\rm k}[n]\rho'^{(n)}_{k,p;\langle u\rangle,f}(\tau) & \\ \quad + \left\{{\rm MAI}^{(n+1)}_{\hat{\alpha}_{k,p}} + 2\left(\sqrt{p_k}\alpha^{(n+1)}_{k,p} + {\rm MAI}^{(n+1)}_{\hat{\alpha}_{{\rm av};k,p}}\right)\Delta^{(n+1)}_k\right\} b_{\rm k}[n+1]\dot{\rho}'^{(n)}_{k,p;\langle u\rangle,f}(\tau), & \text{otherwise} \end{array} \right\}, \quad \tau<0 \tag{20}$$

$$\hat{\breve{\psi}}'^{(n)}_{{\rm SIC};k,p;\langle u\rangle,f}(\tau) = -\left\{ \begin{array}{ll} I^{(n)}_{\hat{\alpha}_{{\rm av};k,p}}\Omega^{(n)}_k b_k[n]\rho'^{(n)}_{k,p;\langle u\rangle,f}(\tau) + I^{(n-1)}_{\hat{\alpha}_{{\rm av};k,p}}\Omega^{(n-1)}_k b_k[n-1]\dot{\rho}'^{(n)}_{k,p;\langle u\rangle,f}(\tau), & \tau\geq 0 \\ I^{(n+1)}_{\hat{\alpha}_{{\rm av};k,p}}\Omega^{(n+1)}_k b_{\rm k}[n+1]\dot{\rho}'^{(n)}_{k,p;\langle u\rangle,f}(\tau), & n=(m+1)G-1 \\ I^{(n)}_{\hat{\alpha}_{{\rm av};k,p}}\Omega^{(n)}_k b_{\rm k}[n]\rho'^{(n)}_{k,p;\langle u\rangle,f}(\tau) + I^{(n+1)}_{\hat{\alpha}_{{\rm av};k,p}}\Omega^{(n+1)}_k b_k[n+1]\dot{\rho}'^{(n)}_{k,p;\langle u\rangle,f}(\tau), & \text{otherwise} \end{array} \right\}, \quad \tau<0 \tag{22}$$

statistics at the uth stage are given as follows:

$$\begin{aligned}\hat{\tilde{Y}}_{\mathrm{SIC}_{\langle u\rangle}} &= P_{\langle u\rangle} b_{\langle u\rangle}[n] + \sqrt{P_{\langle u\rangle}} \\ &\quad \times \mathrm{Re}\left[\mathrm{MAI}_{\mathrm{av};\langle u\rangle} + I_{\mathrm{av};\langle u\rangle}\right] b_{\langle u\rangle}[n] \\ &\quad + \left\{\sqrt{P_{\langle u\rangle}} + \mathrm{Re}\left[\mathrm{MAI}_{\mathrm{av};\langle u\rangle} + I_{\mathrm{av};\langle u\rangle}\right]\right\} \\ &\quad \times \mathrm{Re}\left[\mathrm{MAI}_{\hat{\tilde{b}}_{\mathrm{SIC}_{\langle u\rangle}}} + I_{\hat{\tilde{b}}_{\mathrm{SIC}_{\langle u\rangle}}}\right] \\ &\quad + \mathrm{Im}\left[\mathrm{MAI}_{\mathrm{av};\langle u\rangle} + I_{\mathrm{av};\langle u\rangle}\right] \\ &\quad \times \mathrm{Im}\left[\mathrm{MAI}_{\hat{\tilde{b}}_{\mathrm{SIC}_{\langle u\rangle}}} + I_{\hat{\tilde{b}}_{\mathrm{SIC}_{\langle u\rangle}}}\right]. \end{aligned} \tag{24}$$

1) SIC I—Ordering Based on Average Power: According to the central-limit theorem, $\hat{\tilde{Y}}_{\mathrm{SIC}_{\langle u\rangle}}|b_{\langle u\rangle}$ are assumed as Gaussian-distributed random variables with mean $P_{\langle u\rangle}b_{\langle u\rangle}$ and variance

$$\begin{aligned}\mathrm{Var}\left(\hat{\tilde{Y}}_{\mathrm{SIC}_{\langle u\rangle}}|b_{\langle u\rangle}\right) &\approx \left[P_{\langle u\rangle} + \mathrm{MSE}\left(\hat{\alpha}_{\mathrm{av};\langle u\rangle}\right)\right] \\ &\cdot \left\{\mathrm{Var}\left(\mathrm{Re}\left[\mathrm{MAI}_{\hat{\tilde{b}}_{\mathrm{SIC}_{\langle u\rangle}}}\right]\right) + \mathrm{Var}\left(\mathrm{Re}\left[I_{\hat{\tilde{b}}_{\mathrm{SIC}_{\langle u\rangle}}}\right]\right)\right\} \end{aligned} \tag{25}$$

since the decision statistics are the sum of many variables. This assumption is commonly made in the case of successive cancellation [7]. As shown in the next section, it provides good approximation to the AWGN-dominant systems. The variation of signal power is neglected for simplicity, and the interference components are assumed to be uncorrelated with $b_{\langle u\rangle}$. According to $\lambda'^{(n)}_{k,p;\langle u\rangle,f}(\tau)$, $\hat{\tilde{\varphi}}'_{\mathrm{SIC};k;\langle u\rangle}(\tau)$, and $\hat{\tilde{\psi}}'_{\mathrm{SIC};k;\langle u\rangle}(\tau)$ in (19), (20), and (22), respectively, it is shown in (26), shown at the bottom of the page, where $E[(\hat{\tilde{b}}_{\mathrm{SIC};k})^2] = 4p^{(K)}_{r,\mathrm{TI},k}$, and $p^{(K)}_{r,\mathrm{TI},k}$ denotes the BER of user k [33]. The probability of $\tau \geq 0$ or $\tau < 0$ is equal to 1/2. In addition, only the expected values of the variance of partial code correlations are considered in (26). In addition

$$\begin{aligned}\mathrm{Var}\left(\mathrm{Re}\left[I_{\hat{\tilde{b}}_{\mathrm{SIC}_{\langle u\rangle}}}\right]\right) &= \frac{(\beta_c^2+1)N_0}{4T_b}\left(1/G\left[\frac{3}{4}\cdot\frac{u-1}{\beta_c^2 W(\mathrm{SF})}\right]\right. \\ &\quad \left. + (1-1/G)\left[\frac{u-1}{\beta_c^2 W(\mathrm{SF})}\right] + 1 + \frac{K-1}{W(\mathrm{SF})}\right). \end{aligned} \tag{27}$$

In (26), there are terms coming from channel-estimation errors. Strictly speaking, the BER analysis must be analyzed with the method of robust statistics as far as error detection is concerned [34]. Nevertheless, for simplicity, the error probability for the uth canceled can be approximated as

$$p^{(K)}_{r,\mathrm{TI},\langle u\rangle} \approx Q\left(\sqrt{P^2_{\langle u\rangle}/\mathrm{Var}\left(\hat{\tilde{Y}}_{\mathrm{SIC}_{\langle u\rangle}}|b_{\langle u\rangle}\right)}\right) \tag{28}$$

where $Q(x) = (1/2\pi)\int_x^\infty \exp(-(t^2/2))dt$. The average BER with K users in the system, thus, is $\bar{p}^{(K)}_{r,\mathrm{TI}} = \sum_{k=1}^K p^{(K)}_{r,TI,\langle k\rangle}/K$.

2) SIC II—Ordering Based on RAKE Outputs After G-Bit Cancellation of One User: SIC II finds the next detected user after each cancellation of the currently detected user, i.e., decision statistics of undetected users at each stage are used as ordering basis. For SIC II and SIC III, the BER analysis of the cases with $G > 1$ is very complicated, and thus, only the case of $G = 1$ is performed. Fortunately, as shown in Section V, when G increases, the BER of the three SICs are comparable in the AWGN channel. The error probability for the uth canceled user is given as follows:

$$\begin{aligned}p^{(K)}_{r,\mathrm{TII},\langle u\rangle} &= \frac{(K-1)!}{(K-u)!}\sum_{\langle u\rangle=1}^{K}\sum_{\substack{\langle 1\rangle=1,\\ \langle 1\rangle\neq\langle u\rangle}}^{K}\cdots \\ &\quad \sum_{\substack{\langle u-1\rangle=1,\\ \langle u-1\rangle\neq\langle u\rangle\&\langle 1\rangle\cdots\langle u-2\rangle}}^{K}\ \sum_{\substack{\langle u+1\rangle=u,\\ \langle u+1\rangle\neq\langle 1\rangle\sim\langle u\rangle}}^{K}\cdots\sum_{\substack{\langle K\rangle=K-1,\\ \langle K\rangle\neq\langle 1\rangle\sim\langle K-1\rangle}}^{K} \\ &\quad \cdot \int_0^\infty\int_{-\infty}^\infty\int_{-\infty}^\infty\cdots\int_{-\infty}^\infty f_{\hat{\tilde{Y}}_{\mathrm{SIC}_{\langle u\rangle}}}(x_u) \\ &\quad \times \prod_{k=1}^{k=u-1} f_{g_{\langle u\rangle,\langle k\rangle}}(x_{k+1}-x_k) \\ &\quad \times \left(1 - \left|Q\left(\frac{P_{\langle k\rangle}-x_k}{c(\langle k\rangle,k)}\right) - Q\left(\frac{P_{\langle k\rangle}+x_k}{c(\langle k\rangle,k)}\right)\right|\right) \\ &\quad \cdot \prod_{k=u+1}^{K}\left(\left|Q\left(\frac{P_{\langle k\rangle}-x_u}{c(\langle k\rangle,u)}\right) - Q\left(\frac{P_{\langle k\rangle}+x_u}{c(\langle k\rangle,u)}\right)\right|\right) \\ &\quad \times dx_1 dx_2,\ldots,dxu \end{aligned} \tag{29}$$

$$\begin{aligned}\mathrm{Var}\left(\mathrm{Re}\left[\mathrm{MAI}_{\hat{\tilde{b}}_{\mathrm{SIC}_{\langle u\rangle}}}\right]\right) &= \frac{1}{2\mathrm{SF}}\cdot\left(\frac{1}{G}\left[\frac{3}{4}\left(\sum_{k=\langle u+1\rangle}^{\langle K\rangle}P_k + \sum_{k=\langle 1\rangle}^{\langle u-1\rangle}E\left[|\mathrm{MAI}_{\hat{\alpha}_{\mathrm{av};k}}|^2\right] + \sum_{k=\langle 1\rangle}^{\langle u-1\rangle}P_k E\left[(\hat{\tilde{b}}_{\mathrm{SIC};k})^2\right]\right) + \left(\frac{1}{4}\sum_{k=\langle 1\rangle}^{\langle u-1\rangle}P_k\right)\right]\right. \\ &\quad \left. + \left(1-\frac{1}{G}\right)\left[\sum_{k=\langle u+1\rangle}^{\langle K\rangle}P_k + \sum_{k=\langle 1\rangle}^{\langle u-1\rangle}E\left[|\mathrm{MAI}_{\hat{\alpha}_{\mathrm{av};k}}|^2\right] + \sum_{k=\langle 1\rangle}^{\langle u-1\rangle}P_k E\left[(\hat{\tilde{b}}_{\mathrm{SIC};k})^2\right]\right] + \beta_c^2\sum_{k=1,k\neq\langle u\rangle}^{K}E\left[|\mathrm{MAI}_{\hat{\alpha}_{\mathrm{av};k}}|^2\right]\right) \end{aligned} \tag{26}$$

where

$$c(\nu_1,\nu_2)=[P_{\nu_1}+\mathrm{MSE}(\hat{\alpha}_{a\nu;\nu_1})]^{1/2}\cdot\left[\frac{1}{2\mathrm{SF}}\left(\frac{3}{4}\sum_{k'=1,k'\neq\nu_1\&\sum_{\langle 1\rangle}^{\langle\nu_2-1\rangle}}^{K}P_{k'}+\frac{1}{4}\sum_{k'=1}^{\langle\nu_2-1\rangle}P_{k'}+\frac{3}{4}\sum_{k'=\langle 1\rangle}^{\langle\nu_2-1\rangle}E\left[\left|\mathrm{MAI}_{\hat{\alpha}_{a\nu;k'}}\right|^2\right]\right)+\frac{\beta_c^2}{2\mathrm{SF}}\times\sum_{k'=1,k'\neq\nu_1}^{K}E\left[\left|\mathrm{MAI}_{\hat{\alpha}_{a\nu;k'}}\right|^2\right]+\frac{(\beta_c^2+1)N_0}{4T_b}\times\left(1+\frac{K-1}{W(\mathrm{SF})}+\frac{3}{4}\frac{\nu_2-1}{\beta_c^2W(\mathrm{SF})}\right)\right]^{1/2}\tag{30}$$

where $f_{\hat{\underset{\sim}{Y}}_{\mathrm{SIC}_{\langle u\rangle}}}(x)$ are the probability distribution function (pdf) of Gaussian-distributed random variables $\hat{Y}_{\mathrm{SIC}_{\langle u\rangle}}$ with mean $-P_{\langle u\rangle}$ and variance $c(\langle u\rangle,u)$ when $b_{\langle u\rangle}=-1$. $f_{g_{\nu_1,\nu_2}}(x)$ are the pdf of Gaussian-distributed random variables g_{ν_1,ν_2} with zero-mean and variance equal to

$$\frac{1}{2\mathrm{SF}}\left[P_{\nu_1}+\mathrm{MSE}\left(\hat{\alpha}_{a\nu;\nu_1}\right)\right]\times\frac{3}{4}\left[P_{\nu_2}+\mathrm{MSE}\left(\hat{\alpha}_{a\nu;\nu_2}\right)+\frac{(\beta_c^2+1)N_0}{2\beta_c^2WT_b}\right].\tag{31}$$

It is easy to show that the error probability of the case $b_{\langle u\rangle}=1$ is the same. Equation (29) denotes that the decision variables of the uth detected user falling on $x_1,x_2,\ldots,x_{u-1}$ at the first, second, …, $(u-1)$th stage, respectively, are smaller than those of users $\langle 1\rangle,\langle 2\rangle,\ldots,\langle u-1\rangle$, which are decided to be detected at the first, second, …, $(u-1)$th stage, respectively. When it comes to the uth stage, the decision variables fall on x_u, since interferences from previously detected $u-1$ users are canceled, and there are $K-u$ users whose decision variables are smaller than that of user $\langle u\rangle$ where decision error occurs when $x_u\geq 0$. To simplify the calculation, we assume that $g_{\langle u\rangle,\langle k\rangle}(x_{k+1}-x_k)\approx 1$, since $\mathrm{Var}(g_{\langle u\rangle,\langle k\rangle})$ is small when it is compared to other random variables in (29). Then, the error probability is approximated as

$$p_{r,\mathrm{TII},u}^{(K)}=\frac{(K-1)!}{(K-u)!}\sum_{\langle u\rangle=1}^{K}\sum_{\substack{\langle 1\rangle=1,\\ \langle 1\rangle\neq<u\rangle}}^{K}\cdots\sum_{\substack{\langle u-1\rangle=1,\\ \langle u-1\rangle\neq\langle u\rangle\&\langle 1\rangle\cdots\langle u-2\rangle}}^{K}\times\sum_{\substack{\langle u+1\rangle=u,\\ \langle u+1\rangle\neq\langle 1\rangle\sim\langle u\rangle}}^{K}\cdots\sum_{\substack{\langle K\rangle=K-1,\\ \langle K\rangle\neq\langle 1\rangle\sim\langle K-1\rangle}}^{K}\int_0^{\infty}f_{\hat{\underset{\sim}{Y}}_{\mathrm{SIC}_{\langle u\rangle}}}(x)\cdot\prod_{k=1}^{k=u-1}\left(1-\left|Q\left(\frac{P_{\langle k\rangle}-x}{c(\langle k\rangle,k)}\right)Q\left(\frac{P_{\langle k\rangle}+x}{c(\langle k\rangle,k)}\right)\right|\right)\times\prod_{k=u+1}^{K}\left(\left|Q\left(\frac{P_{\langle k\rangle}-x}{c(\langle u\rangle,k)}\right)Q\left(\frac{P_{\langle k\rangle}+x}{c(\langle u\rangle,k)}\right)\right|\right)dx\tag{32}$$

The average BER of SIC II is given by $\bar{p}_{r,\mathrm{TII}}^{(K)}=\sum_{k=1}^{K}p_{r,\mathrm{TII},\langle k\rangle}^{(K)}/K$.

3) SIC III—Ordering Based on RAKE Outputs at First Stage in Each G-Bit Interval: In SIC III, user data is detected and canceled according to descending signal strength at the correlator outputs of the first stage, i.e., decision statistics of all users at the first stage are used as the ordering basis. Thus, the error probability for the uth canceled user is modified to

$$p_{r,\mathrm{TIII},\langle u\rangle}^{(K)}=\frac{(K-1)!}{(u-1)!(K-u)!}\sum_{\langle u\rangle=1}^{K}\sum_{\substack{\langle 1\rangle=1,\\ \langle 1\rangle\neq\langle u\rangle}}^{K}\sum_{\substack{\langle 2\rangle=2,\\ \langle 2\rangle\neq\langle u\rangle\&\langle 1\rangle}}^{K}\cdots\sum_{\substack{\langle u-1\rangle=u-1,\\ \langle u-1\rangle\neq\langle u\rangle\&\langle 1\rangle\sim\langle u-2\rangle}}^{K}\sum_{\substack{\langle u+1\rangle=u,\\ \langle u+1\rangle\neq\langle 1\rangle\sim\langle u\rangle}}^{K}\cdots\sum_{\substack{\langle K\rangle=K-1,\\ \langle K\rangle\neq\langle 1\rangle\sim\langle K-1\rangle}}^{K}\times\int_0^{\infty}\int_{-\infty}^{\infty}f_{\hat{\underset{\sim}{Y}}_{\mathrm{SIC}_{\langle u\rangle}}}(x_2)\sum_{k=1}^{u-1}f_{g_{\langle u\rangle,\langle k\rangle}}(x_2-x_1)\cdot\prod_{k=1}^{u-1}\left(1-\left|Q\left(\frac{P_{\langle k\rangle}-x_1}{c\left(\langle k\rangle,1\right)}\right)-Q\left(\frac{P_{\langle k\rangle}+x_1}{c\left(\langle k\rangle,1\right)}\right)\right|\right)\times\prod_{k=u+1}^{K}\left(\left|Q\left(\frac{P_{\langle k\rangle}-x_1}{c\left(\langle k\rangle,1\right)}\right)-Q\left(\frac{P_{\langle k\rangle}+x_1}{c\left(\langle k\rangle,1\right)}\right)\right|\right)dx_1dx_2.\tag{33}$$

Equation (33) indicates that a user with decision variables $\hat{\underset{\sim}{Y}}_{\langle u\rangle}=c(\langle u\rangle,1)$, which have fallen on x_1 at the first stage, was decided to be canceled in the uth stage, since there are $u-1$ users having larger value of decision variables and there are $K-u$ users with smaller value of decision variables than user $\langle u\rangle$. When it comes to the uth stage, the value of decision variables becomes x_2 since interferences from previously detected $u-1$ users are canceled, and the decision error occurs when $x_2\geq 0$ in the case of $b_{\langle u\rangle}=-1$. The decision errors of previously detected users are ignored for simplicity in both SIC II and SIC III. The average BER for a system with K users is $\bar{p}_{r,\mathrm{TIII}}^{(K)}=\sum_{k=1}^{K}p_{r,\mathrm{TIII},\langle k\rangle}^{(K)}/K$.

From the above analyses, channel-estimation errors are shown to lead to nonlinear influence on the decision statistics. Analytical methods used in SIC II and SIC III can be viewed as the modification of the order statistics [35], where the ordering basis of SIC II changes after each cancellation.

V. Results and Discussions

The general simulation parameters used are summarized in Table II according to Third-Generation Partnership Project standard [23], if they are not explicitly specified in the text. β_c is chosen for the optimal BER according to the simulation results. The average SNR denotes the average of energy per bit of each user divided by noise variance. The chip resolution

TABLE II
SIMULATION PARAMETERS

Symbol	Quantity		
$1/T_c$	Chip Rate	3.84Mhz	
f_c	Carrier Frequency	2 GHz	
SF	Spreading Factor	16	
$1/T_b$	Bit Rate	240 Kbps	
N	Scramble Sequence Length	38400 Chips	
NT_c	Frame Period	10 ms	
β_c	Pilot-to-Traffic Amplitude Ratio	AWGN	7/15
		Fading Channels	10/15
K	User Number	8	
SNR	Average SNR per Bit	AWGN	15 dB
		Fading Channels	20 dB
	Multipath Fading Channel Conditions	See TABLE. 3	

in AWGN is chosen to be one chip, since chip synchronous is assumed, while the general chip resolution in multipath fading environment is 0.25 chips, where chip asynchronous is assumed.

A. Channel Estimation

Fig. 6 shows the analytical and simulated results of MSE with $W = 64$ and $W = 128$ over flat Rayleigh fading channels where Doppler shift $f_d = 222$ Hz, corresponding to a vehicle speed of 120 km/h. The analytical MSE provides good approximation to the simulated MSE. It is shown that large β_c results in better channel estimates, since λ from other users in (4) is alleviated in proportion to the reciprocal of β_c.

B. Data Detection

1) AWGN Channel: In Fig. 7, the influence of various G and PDR are examined in AWGN channel. The analytical results of $G = 1$ and $G = 2400$ are shown in dotted line where SIC I with $G = 2400$ is used to approximate SIC II and SIC III with $G = 2400$, and it shows good approximation to the simulated results. The BER difference of the three SICs is explicit when G is small and PDR is close to unity, and SIC II outperforms the other two SICs in this situation. As G or PDR increases, all SICs have almost the same performance. This is because the difference in the cancellation order of the three SICs is less and less as PDR or G increases.

Fig. 8(a) shows the individual BER of the uth detected user with eight active users in the system. When $G = 1$, we find that the late-detected users of SIC I outperform those of SIC II and SIC III. Nevertheless, the early detected users of SIC II and SIC III perform much better than those of SIC I. Thus, SIC II and SIC III still outperform SIC I after averaging, as shown in Fig. 8(b). Fig. 8(b) shows the average BER versus user number for the three SICs when $G = 1$ and 2400. Only SIC I with $G = 2400$ is presented since it is shown in Fig. 7 that the three SICs have almost the same BER. All users in SIC II in Fig. 8(a), except the last one, outperform those in SIC III, and thus, the average BER of SIC II in Fig. 8(b) is lower than that of SIC III.

In Fig. 9, the BER with different PDRs and SNRs are examined when $G = 1$ and $G = 2400$. β_c is chosen for optimal BER of the corresponding SNR. In this paper, SIC without PCSR denotes that the pilot-channel signal are not removed first from the received signal, but they are removed accompanying with the data-channel signal of the corresponding user. Thus, SIC with PCSR outperforms SIC without PCSR only at the cost of demanding slightly more latency. As SNR increases, the benefit of SIC with PCSR becomes obvious, and all SICs with $G = 2400$ outperform SIC II with $G = 1$. For $G = 2400$, as shown in Fig. 9(d), increasing SNR also results in the increasing in PDR for the optimum BER. The reason is that MAI dominates the BER at high SNR, and increasing PDR can alleviate MAI from early detected users.

In Fig. 10, we examine the influence of pilot-to-traffic amplitude ratio (β_c). For the last two lines in Fig. 10(a) and (b), the PDRs are chosen for the minimum BER for the SIC with PCSR when $G = 2400$, i.e., PDR $= 1.3(K = 8)$ and PDR $= 1.1(K = 16)$ for all SICs. In Fig. 6, it is shown that large β_c brings better channel estimates. However, large β_c also leads to poor data detection since the percentage of transmitted power for data signal decreases, and MAI from pilot signal increases. It is shown that SIC with PCSR can dramatically alleviate MAI from pilot signal, particularly when β_c increases. In addition, SIC with PCSR is less sensitive to the variation of β_c in both moderately loaded case in Fig. 10(a) and heavily loaded case in Fig. 10(b).

2) Multipath Fading Channels: Four cases of propagation conditions for multipath fading environments used in the following are presented in Table III. It is assumed that all paths are tracked and combined in the RAKE receiver, i.e., $F = P$.

In Fig. 11, the three SICs in all considered channels perform much better than the RAKE receiver. The best BER occurs at PDR $= 1.3$ for SIC I in all cases, while it occurs at PDR $= 1.0$ for SIC II and SIC III in channel Case 1 and channel Case 2, and at PDR $\neq 1.0$ in channel Case 3 and channel Case 4. SIC II performs slightly better than SIC III when PDR is close to unity and G is small, and they both achieve better BER than SIC I. This is because SIC II and SIC III have the ability to track channel variation and SIC I does not.

In Fig. 12, the BER is investigated with channel estimation where $W = 128$. The timing-estimation errors are modeled as Gaussian-distributed random variables with zero-mean and variance 0.0625 (two samples) at 1/32 chips resolution, where 95% of the probability mass is concentrated within ± 4 samples [37]. The simulated results are similar to those in Fig. 11 except that the best BER occurs at PDR $= 1.0$ for SIC II and SIC III in all channel cases.

Fig. 13 indicates the BER of individual user in different cancellation order with the PDR for the optimum BER in each SIC in channel Case 3. For SIC I in Fig. 13(a), influences of G are obvious only when G is small. For SIC II in Fig. 13(b) and SIC III in Fig. 13(c), the early canceled users have smaller BER than that of the late canceled users for small G. As $G > 1000$, their BER becomes worse than SIC I where the early canceled users have larger BER than that of the late canceled

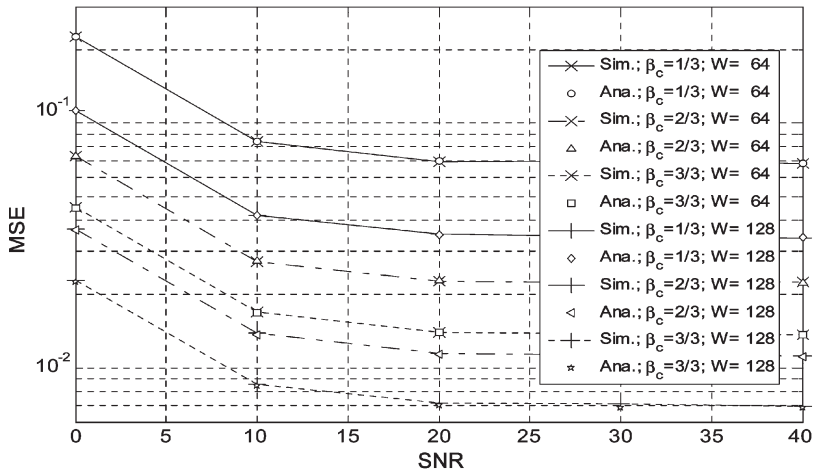

Fig. 6. MSE of channel estimates with various SNRs, flat Rayleigh fading channel, PDR $= 1.0$, and $G = 1$.

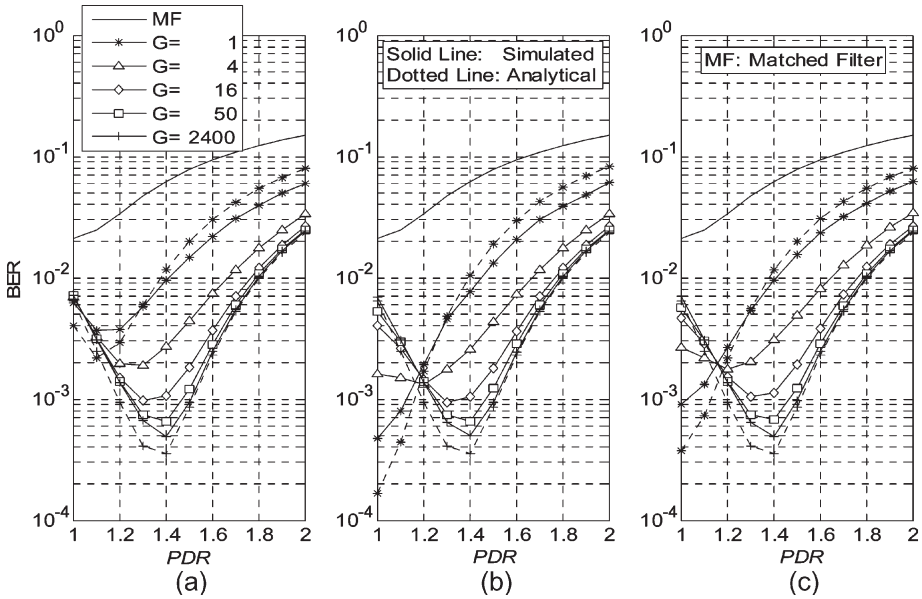

Fig. 7. BER versus PDR with different grouping interval G for (a) SIC I, (b) SIC II, and (c) SIC III. AWGN, known channel parameters, with PCSR.

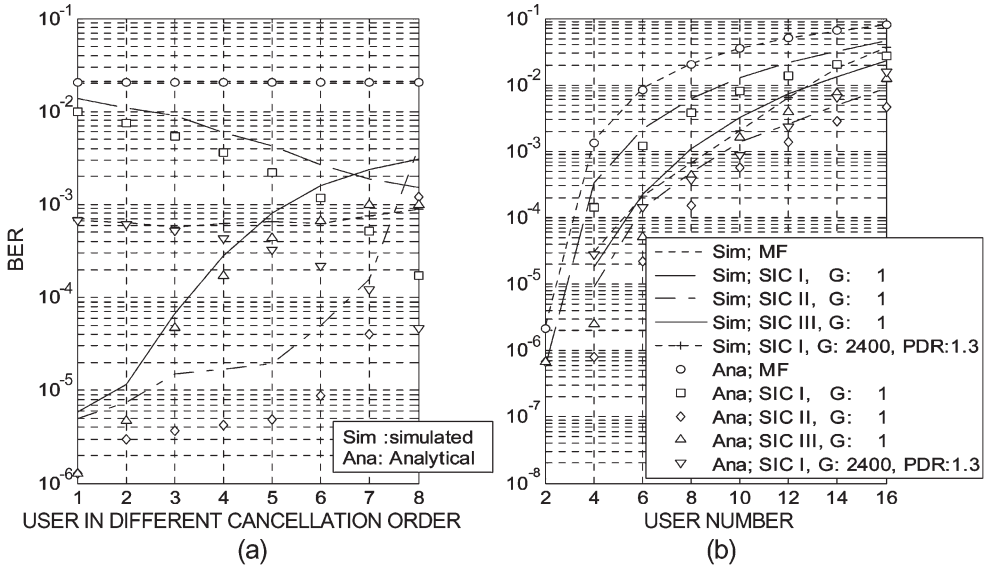

Fig. 8. Simulated and analytical results of SICs with PCSR (a) individual BER in an eight-user system and (b) average BER.

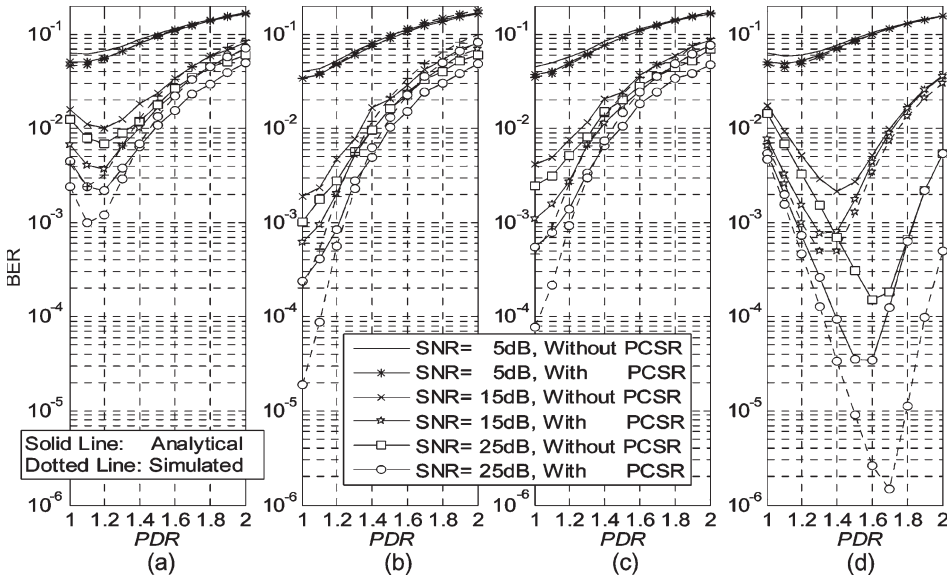

Fig. 9. BER comparison with different PDRs and SNRs with/without PCSR for (a) SIC I with $G = 1$, (b) SIC II with $G = 1$, (c) SIC III with $G = 1$, and (d) SIC I with $G = 2400$. AWGN, channel estimation with $W = 128$.

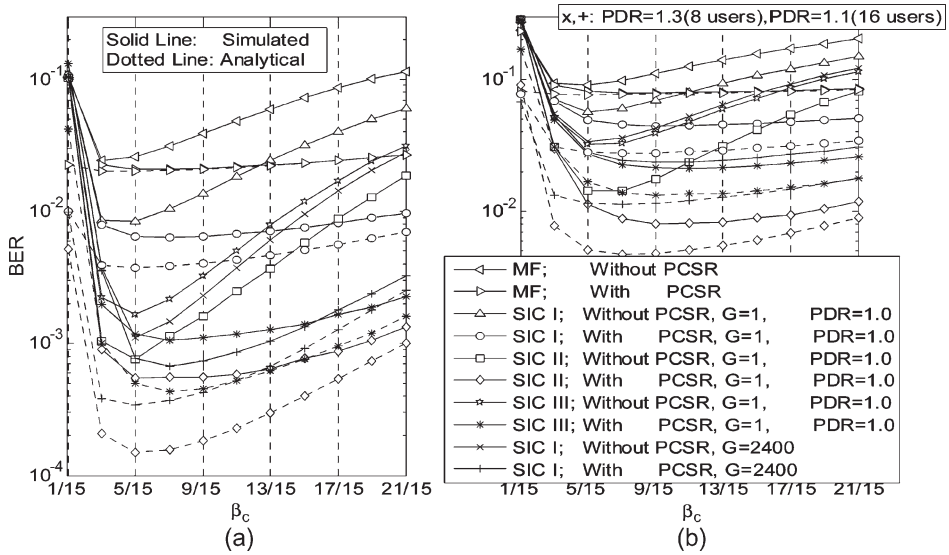

Fig. 10. BER versus β_c with/without PCSR when there are (a) eight users and (b) 16 users in the system. AWGN, channel estimation with $W = 128$.

TABLE III
PROPAGATION CONDITIONS FOR MULTIPATH FADING ENVIRONMENTS [36]

Case 1, speed 3 km/h		Case 2, speed 3 km/h	
Relative Delay [ns]	Average Power [dB]	Relative Delay [ns]	Average Power [dB]
0	0	0	0
976	-10	976	0
		20000	0
Case 3, 120 km/h		Case 4, 250 km/h	
Relative Delay [ns]	Average Power [dB]	Relative Delay [ns]	Average Power [dB]
0	0	0	0
260	-3	260	-3
521	-6	521	-6
781	-9	781	-9

users. In addition, SIC II slightly outperforms SIC III when G is small.

The BER versus β_c over all channel cases are given in Fig. 14, where G and PDR are selected for the best BER, i.e., $G = 2400$ in channel Case 1 and channel Case 2, $G = 32$ in channel Case 3, and $G = 16$ in channel Case 4 for all SICs. Similar to the results shown in Fig. 10 for AWGN channel, the PCSR helps to improve BER and increase β_c for the optimum BER. SIC II and SIC III still perform much better than SIC I. Moreover, SIC II and SIC III have similar performance.

In Fig. 15, the BER for various channel cases are examined. According to the results in Fig. 11, the PDRs for the minimum BER of each SIC are chosen. In channel Case 1 and channel Case 2, the one-frame long grouping interval, i.e., $G = 2400$, results in the best BER for all SICs. However, in channel Case 3 and channel Case 4, the optimum BER for SIC II and SIC III occur at about $G = 100$ and $G = 50$, respectively. Among all

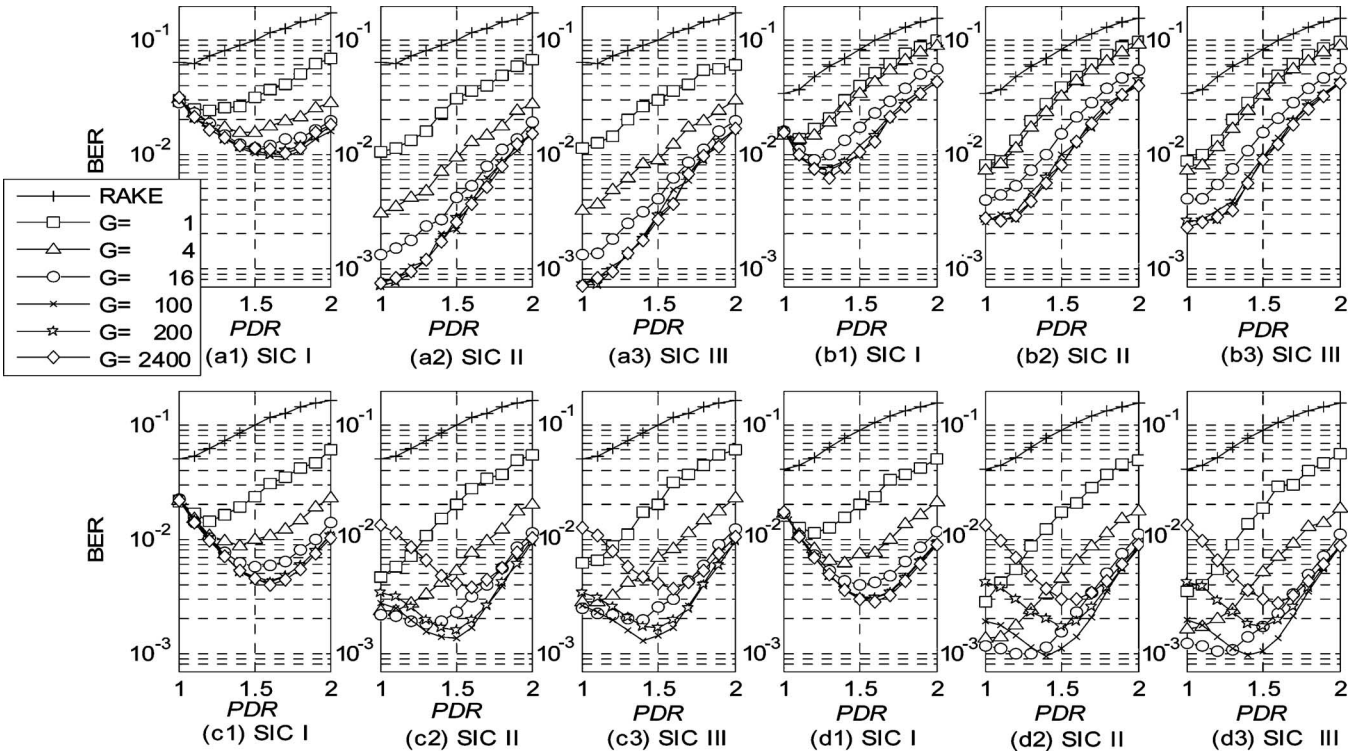

Fig. 11. BER versus PDR for the three SICs in multipath fading channels. (a) Case 1. (b) Case 2. (c) Case 3. (d) Case 4. With PCSR, known channel parameters.

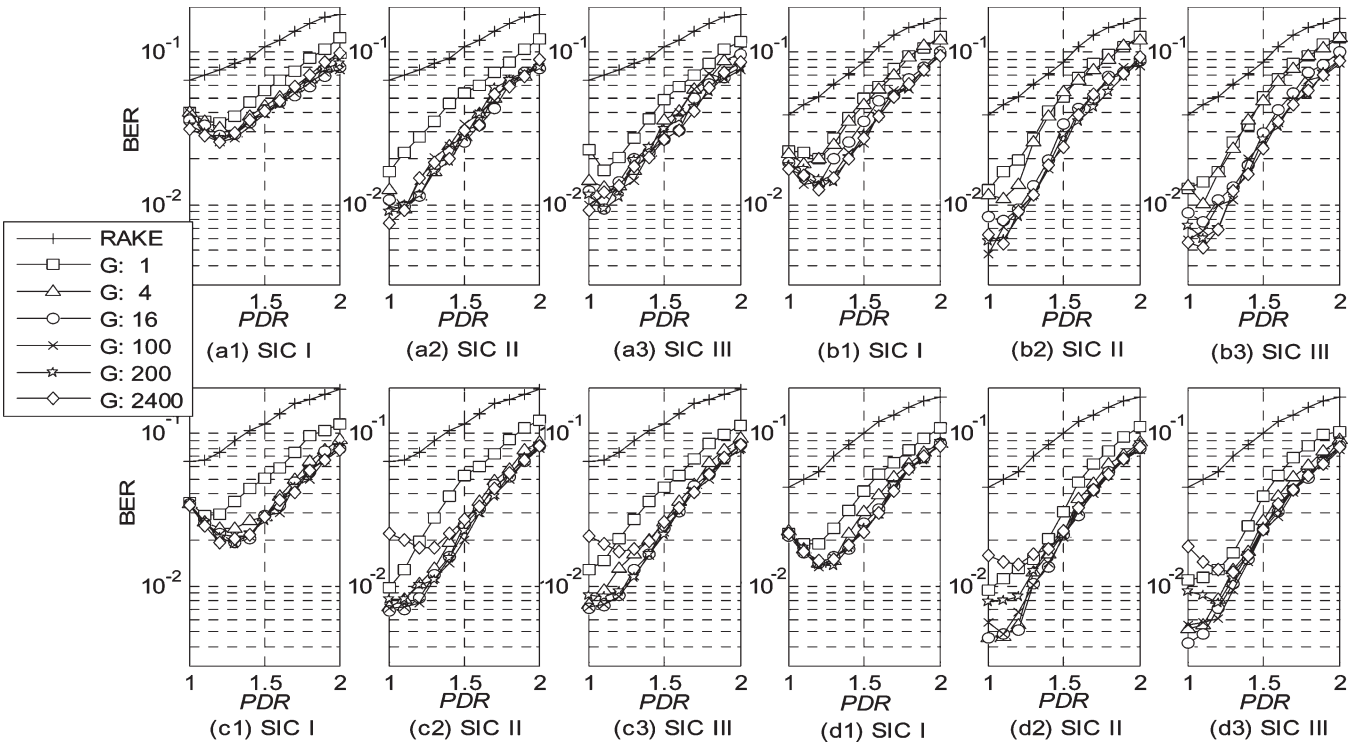

Fig. 12. BER versus PDR for the three SICs in multipath fading channels. (a) Case 1. (b) Case 2. (c) Case 3. (d) Case 4. Channel estimation with $W = 128$ and timing-estimation error with variance two samples at 1/32 chips resolution.

channel cases, SIC II and SIC III outperform SIC I, and except in channel Case 3 and channel Case 4 when G is small than about 20 with channel estimation, these two SICs almost have the same BER. It is worthy to note that SIC II and SIC III, with properly chosen G as PDR $= 1$, are suitable for fast fading channels such as channel Case 4.

From the above simulations and analyses, we find the following.

1) The SIC with PCSR can achieve better BER than that without PCSR when β_c is large in both AWGN and selective fading channels. The optimal β_c for SIC with PCSR is larger than that without PCSR. Larger β_c also

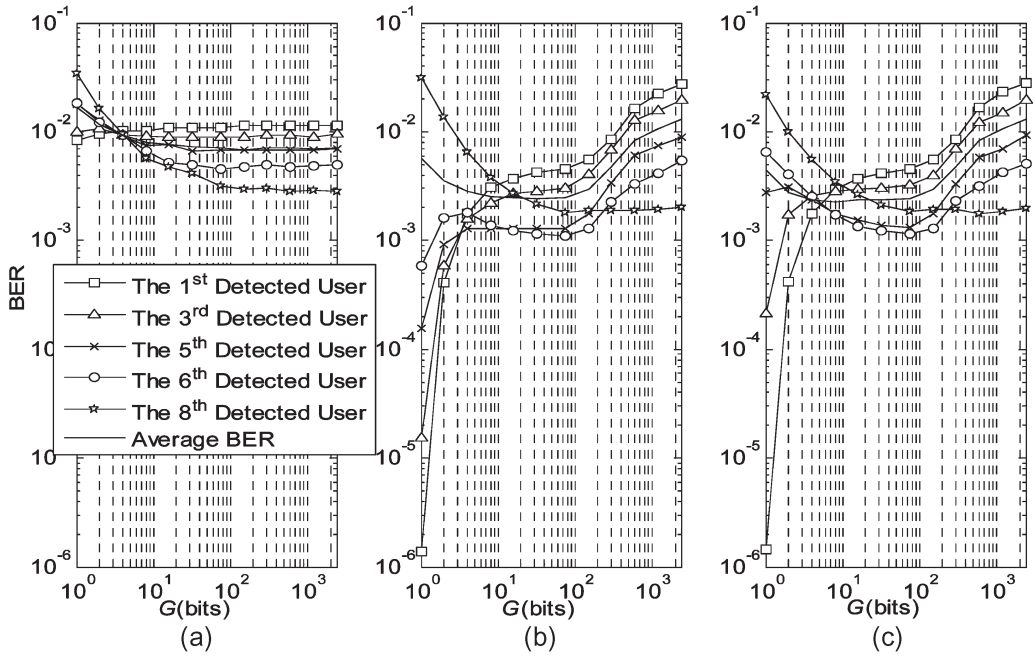

Fig. 13. BER versus grouping interval G for user in different detection order for (a) SIC I with PDR $= 1.3$, (b) SIC II with PDR $= 1.0$, and (c) SIC III with PDR $= 1.0$. Channel Case 3, known channel parameter, with PCSR.

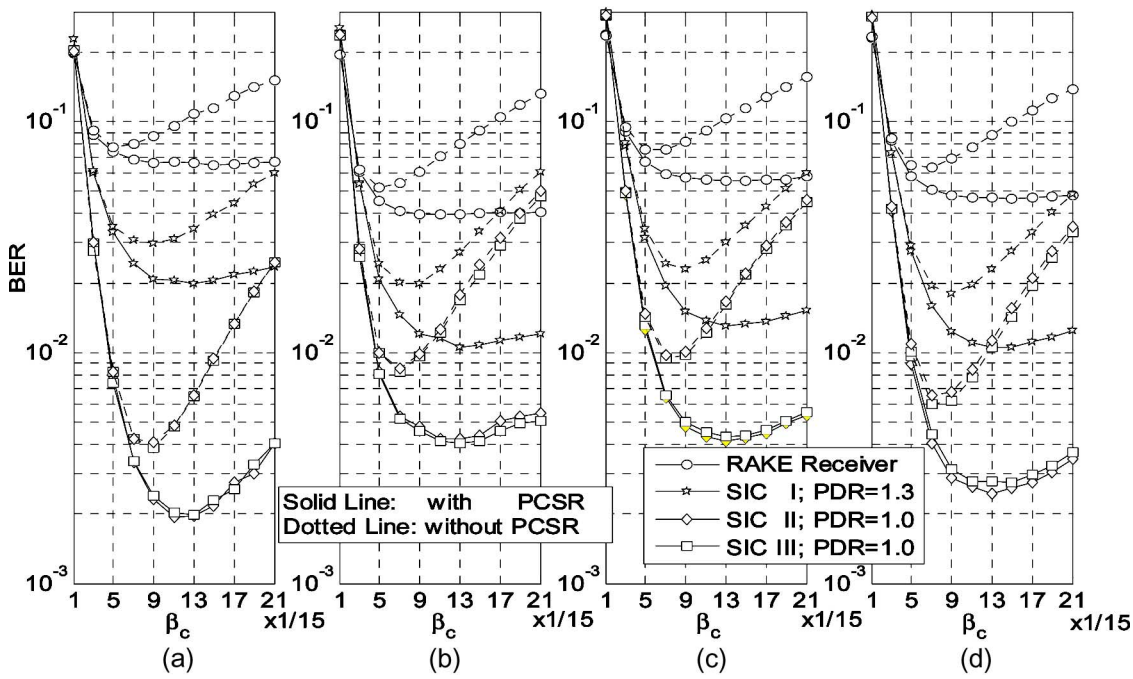

Fig. 14. BER versus β_c for multipath fading channels. (a) Case 1. (b) Case 2. (c) Case 3. (d) Case 4. Channel estimation with $W = 128$.

implies less timing-estimation error, which is critical in most communication systems.

2) The benefit of detecting and canceling a group of G-bit in AWGN channel becomes obvious when noise and MAI decrease. The reason has been mentioned in Section III-B. The relationship between f_d and the optimal G of SIC III-like SIC in multirate systems in multipath fading channels is examined in the study in [38], where the optimal G is shown inversely proportional to f_d in fading environment. In addition, larger G results in better BER in SIC I in all fading channel cases since the detection order is not affected by G.

3) When the noise (including estimation errors) and MAI increase, the PDR for the optimum BER in AWGN channel becomes closer to one as explained in Fig. 9. For SIC I over fading channels, it is shown that the optimum BER always occurs at PDR $\neq 1$, since detection order is fixed. As for SIC II and SIC III, whether PDR of the optimum BER is equal to unity depends on the channel condition.

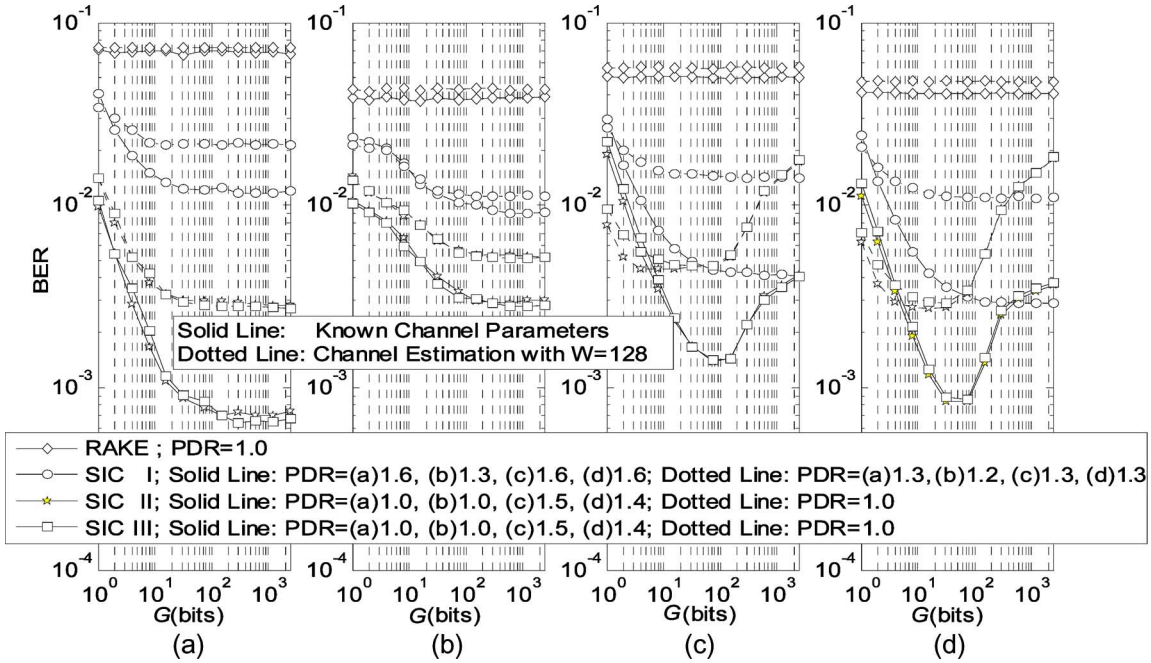

Fig. 15. BER versus grouping interval G for multipath fading channels. (a) Case 1. (b) Case 2. (c) Case 3. (d) Case 4. With PCSR.

4) The BER of SIC I is inferior to the other two SICs when G is small. For SIC II and SIC III, they perform almost the same in both AWGN channel and fading channel when G or PDR is larger than one. In the view of BER, SIC II would be a good choice when it is applied to a heavily loaded system over AWGN channel with $G = 1$ or when G for the optimum BER is smaller than 16[1] over multipath fading channels.

VI. Conclusion

In this paper, we investigate a pilot-channel-aided SIC scheme for uplink WCDMA systems. The scheme alleviates the interference from traffic-channel as well as pilot-channel signals of other users. We discuss SIC with three ordering methods and compare their corresponding architectures as well as processing delays and computational complexities. In addition to showing the superiority over the conventional RAKE receiver, the influence of ordering method, pilot-to-traffic amplitude ratio, grouping interval, PDR, and channel- and timing-estimation errors are jointly examined and discussed. It is found out that ordering based on average power (SIC I) requires the least computational complexity at the expense of BER when grouping interval is small, and it seems to be suitable for AWGN channels with moderate loading. Ordering based on RAKE outputs after each cancellation of grouping-interval bits of one user (SIC II) outperforms ordering based on RAKE outputs at initial stage in each grouping interval (SIC III) when grouping interval is small. But SIC II has the highest computational complexity and the largest processing delay among all SICs. SIC III is proposed to be a better choice over multipath fading channels when BER and computational complexity are jointly concerned.

[1]With the simulation parameters used in this paper, $G = 16$ when the vehicle speed is at about 250 km/hr.

Appendix

We are to derive $\mathrm{MAI}_{\hat{\alpha}J,f}^{(n)}$ in (4) by first considering the following expression:

$$\frac{1}{2T_b}\int_{nT_b+\tau_J}^{(n+1)T_b+\tau_J} b_k(t-\tau_{k,p})C_O(t-\tau_{k,p}) \times C_k(t-\tau_{k,p})C_J^*(t-\tau_{J,f})dt. \quad \text{(A1)}$$

After taking definitions of $b_k(t)$, $C_O(t)$, and $C_k(t)$ into (A1), it becomes

$$\frac{1}{2T_b}\sum_n\sum_m\sum_q b_k[n]c_O[q]c_k[q]c_J^*[m] \cdot \int_{n\mathrm{SF}T_c+\tau_{J,f}}^{(n+1)\mathrm{SF}T_c+\tau_{J,f}} p(t-qT_c-\tau_{k,p}) \times p\left(t-qT_c-\tau_{k,p}\right)p\left(t-mT_c-\tau_{J,p}\right)dt$$

where n, m, and q are all nonzero integers. With the timing-delay illustration shown in Fig. 2, we define $\tau_{k,p} = q'T_c + \tau'_{k,p}, \tau'_{k,p} < T_c$ and $\tau_{J,f} = m'T_c + \tau'_{J,f}, \tau'_{J,f} < T_c$ for $q' \geq 0$, $m' \geq 0$, and $\tau'_{k,p} - \tau'_{J,f} = \tau'_{k,p;J,f}$. In the following, we take $\tau = \tau_{k,p;J,f}$ and $\tau' = \tau'_{k,p;J,f}$ for notational simplicity.

If $\tau = iT_c + \tau'$ for $0 \le \tau'_{k,p;J,f} < T_c$, where i is a nonzero integer, when $\tau \ge 0$, (A1) become

$$\begin{aligned}&\frac{1}{2T_b} b_k[n] \sum_m \sum_q c_O[q] c_k[q] c_J^*[m] \\ &\quad \times \int_{n\mathrm{SF}T_c+\tau}^{(n+1)\mathrm{SF}T_c} p\left(\lambda - (q-m+i)T_c - \tau'\right) p(\lambda) d\lambda \\ &\quad + \frac{1}{2T_b} b_k[n-1] \sum_m \sum_q c_O[q] c_k[q] c_J^*[m] \\ &\quad \times \int_{n\mathrm{SF}T_c}^{n\mathrm{SF}T_c+\tau} p\left(\lambda - (q-m+i)T_c - \tau'\right) p(\lambda) d\lambda \quad \text{(A2)}\end{aligned}$$

where $\lambda = t - mT_c$. We can find that $|(q-m+i)T_c + \tau'| < T_c$, such that the integral is nonzero, i.e., $-\tau'/T_c + m - i - 1 < q < -\tau'/T_c + m - i + 1$. Thus, (A2) becomes

$$\begin{aligned}&\frac{1}{2\mathrm{SF}} \frac{T_c - \tau'}{T_c} \left\{ b_k[n] \sum_{m=n\mathrm{SF}+i}^{(n+1)\mathrm{SF}-1} c_O[m-i] c_k[m-i] c_J^*[m] \right. \\ &\qquad \left. + b_k[n-1] \sum_{m=n\mathrm{SF}}^{n\mathrm{SF}+i-1} c_O[m-i] c_k[m-i] c_J^*[m] \right\}\end{aligned}$$

when $q = m - i$, and

$$\begin{aligned}&\frac{1}{2\mathrm{SF}} \frac{\tau'}{T_c} \left\{ b_k[n] \sum_{m=n\mathrm{SF}+i+1}^{(n+1)\mathrm{SF}-1} c_O[m-i-1] c_k[m-i-1] c_J^*[m] \right. \\ &\qquad \left. + b_k[n-1] \sum_{m=n\mathrm{SF}}^{n\mathrm{SF}+i} c_O[m-i-1] c_k[m-i-1] c_J^*[m] \right\}\end{aligned}$$

when $q = m - i - 1$. Similarly, when $\tau < 0$, $\tau = -iT_c + \tau'$, where $0 \ge \tau' > -T_c$ and (A1) become

$$\begin{aligned}&\frac{1}{2T_b} b_k[n] \sum_m \sum_q c_O[q] c_k[q] c_J^*[m] \\ &\quad \times \int_{n\mathrm{SF}T_c}^{(n+1)\mathrm{SF}T_c+\tau} p\left(\lambda - (q-m-i)T_c - \tau'\right) p(\lambda) d\lambda \\ &\quad + \frac{1}{2T_b} b_k[n+1] \sum_m \sum_q c_O[q] c_k[q] c_J^*[m] \\ &\quad \times \int_{(n+1)\mathrm{SF}T_c+\tau}^{(n+1)\mathrm{SF}T_c} p\left(\lambda - (q-m-i)T_c - \tau'\right) p(\lambda) d\lambda \quad \text{(A3)}\end{aligned}$$

where $\lambda = t - mT_c$. We can find that $|(q-m-i)T_c + \tau'| < T_c$, such that the integral is nonzero, i.e., $-\tau'/T_c + m + i - 1 < q < -\tau'/T_c + m + i + 1$. When $q = m + i$, (A3) becomes

$$\begin{aligned}&\frac{1}{2\mathrm{SF}} \frac{T_c - \tau'}{T_c} \left\{ b_k[n] \sum_{m=n\mathrm{SF}}^{(n+1)\mathrm{SF}-i-1} c_O[m+i] c_k[m+i] c_J^*[m] \right. \\ &\qquad \left. + b_k[n+1] \sum_{m=(n+1)\mathrm{SF}-i}^{(n+1)\mathrm{SF}-1} c_O[m+i] c_k[m+i] c_J^*[m] \right\}\end{aligned}$$

when $q = m + i + 1$, (A3) becomes

$$\begin{aligned}&\frac{1}{2\mathrm{SF}} \frac{\tau'}{T_c} \left\{ b_k[n] \sum_{m=n\mathrm{SF}-1}^{(n+1)\mathrm{SF}-i-2} c_O[m+i+1] \right. \\ &\qquad \times c_k[m+i+1] c_J^*[m] + b_k[n+1] \\ &\qquad \left. \times \sum_{(n+1)\mathrm{SF}-i-1}^{(n+1)\mathrm{SF}-1} c_O[m+i+1] c_k[m+i+1] c_J^*[m] \right\}.\end{aligned}$$

$$\rho^{(n)}_{k,p;J,f}(\tau) = \begin{cases} \frac{1}{2\mathrm{SF}} \left\{ \sum_{m=n\mathrm{SF}+i}^{(n+1)\mathrm{SF}-1} \frac{T_c - \tau'}{T_c} c_O[m-i] c_k[m-i] c_J^*[m] + \sum_{m=n\mathrm{SF}+i+1}^{(n+1)\mathrm{SF}-1} \frac{\tau'}{T_c} c_O[m-i-1] c_k[m-i-1] c_J^*[m] \right\}, & \tau \ge 0 \\ \frac{1}{2\mathrm{SF}} \left\{ \sum_{m=n\mathrm{SF}}^{(n+1)\mathrm{SF}-i-1} \frac{T_c - \tau'}{T_c} c_O[m+i] c_k[m+i] c_J^*[m] + \sum_{m=n\mathrm{SF}}^{(n+1)\mathrm{SF}-i-2} \frac{\tau'}{T_c} c_O[m+i+1] c_k[m+i+1] c_J^*[m] \right\}, & \tau < 0 \end{cases} \quad \text{(A4)}$$

$$\dot{\rho}^{(n)}_{k,p;J,f}(\tau) = \begin{cases} \frac{1}{2\mathrm{SF}} \left\{ \sum_{m=n\mathrm{SF}}^{n\mathrm{SF}+i-1} \frac{T_c - \tau'}{T_c} c_O[m-i] c_k[m-i] c_J^*[m] + \sum_{m=n\mathrm{SF}}^{n\mathrm{SF}+i} \frac{\tau'}{T_c} c_O[m-i-1] c_k[m-i-1] c_J^*[m] \right\}, & \tau \ge 0 \\ \frac{1}{2\mathrm{SF}} \left\{ \sum_{m=(n+1)\mathrm{SF}-i}^{(n+1)\mathrm{SF}-1} \frac{T_c - \tau'}{T_c} c_O[m+i] c_k[m+i] c_J^*[m] \right. & \\ \qquad \left. + \sum_{m=(n+1)\mathrm{SF}-i-1}^{(n+1)\mathrm{SF}-1} \frac{\tau'}{T_c} c_O[m+i+1] c_k[m+i+1] c_J^*[m] \right\}, & \tau < 0 \end{cases} \quad \text{(A5)}$$

$$\gamma_{k,p;J,f}^{(n)}(\tau)=\begin{cases}\frac{1}{2\mathrm{SF}}\left\{\sum\limits_{m=n\mathrm{SF}+i}^{(n+1)\mathrm{SF}-1}\frac{T_c-\tau'}{T_c}c_k[m-i]c_J^*[m]+\sum\limits_{m=n\mathrm{SF}+i+1}^{(n+1)\mathrm{SF}-1}\frac{\tau'}{T_c}c_k[m-i-1]c_J^*[m]\right\}, & \tau\geq 0\\ \frac{1}{2\mathrm{SF}}\left\{\sum\limits_{m=n\mathrm{SF}}^{(n+1)\mathrm{SF}-i-1}\frac{T_c-\tau'}{T_c}c_k[m+i]c_J^*[m]+\sum\limits_{m=n\mathrm{SF}}^{(n+1)\mathrm{SF}-i-2}\frac{\tau'}{T_c}c_k[m+i+1]c_J^*[m]\right\}, & \tau<0\end{cases} \tag{A6}$$

$$\dot{\gamma}_{k,p;J,f}^{(n)}(\tau)=\begin{cases}\frac{1}{2\mathrm{SF}}\left\{\sum\limits_{m=n\mathrm{SF}}^{n\mathrm{SF}+i-1}\frac{T_c-\tau'}{T_c}c_k[m-i]c_J^*[m]+\sum\limits_{m=n\mathrm{SF}}^{n\mathrm{SF}+i}\frac{\tau'}{T_c}c_k[m-i-1]c_J^*[m]\right\}, & \tau\geq 0\\ \frac{1}{2\mathrm{SF}}\left\{\sum\limits_{m=(n+1)\mathrm{SF}-i}^{(n+1)\mathrm{SF}-1}\frac{T_c-\tau'}{T_c}c_k[m+i]c_J^*[m]+\sum\limits_{m=(n+1)\mathrm{SF}-i-1}^{(n+1)\mathrm{SF}-1}\frac{\tau'}{T_c}c_k[m+i+1]c_J^*[m]\right\}, & \tau<0\end{cases} \tag{A7}$$

$$\rho_{k,p;J,f}^{\prime(n)}(\tau)=\begin{cases}\frac{1}{2\mathrm{SF}}\left\{\sum\limits_{m=n\mathrm{SF}+i}^{(n+1)\mathrm{SF}-1}\frac{T_c-\tau'}{T_c}c_O[m-i]c_O[m]c_k[m-i]c_J^*[m]\right.\\ \qquad\left.+\sum\limits_{m=n\mathrm{SF}+i+1}^{(n+1)\mathrm{SF}-1}\frac{\tau'}{T_c}c_O[m-i-1]c_O[m]c_k[m-i-1]c_J^*[m]\right\}, & \tau\geq 0\\ \frac{1}{2\mathrm{SF}}\left\{\sum\limits_{m=n\mathrm{SF}}^{(n+1)\mathrm{SF}-i-1}\frac{T_c-\tau'}{T_c}c_O[m+i]c_O[m]c_k[m+i]c_J^*[m]\right.\\ \qquad\left.+\sum\limits_{m=n\mathrm{SF}}^{(n+1)\mathrm{SF}-i-2}\frac{\tau'}{T_c}c_O[m+i+1]c_O[m]c_k[m+i+1]c_J^*[m]\right\}, & \tau<0\end{cases} \tag{A8}$$

$$\dot{\rho}_{k,p;J,f}^{\prime(n)}(\tau)=\begin{cases}\frac{1}{2\mathrm{SF}}\left\{\sum\limits_{m=n\mathrm{SF}}^{n\mathrm{SF}+i-1}\frac{T_c-\tau'}{T_c}c_O[m-i]c_O[m]c_k[m-i]c_J^*[m]\right.\\ \qquad\left.+\sum\limits_{m=n\mathrm{SF}}^{n\mathrm{SF}+i}\frac{\tau'}{T_c}c_O[m-i-1]c_O[m]c_k[m-i-1]c_J^*[m]\right\}, & \tau\geq 0\\ \frac{1}{2\mathrm{SF}}\left\{\sum\limits_{m=(n+1)\mathrm{SF}-i}^{(n+1)\mathrm{SF}-1}\frac{T_c-\tau'}{T_c}c_O[m+i]c_O[m]c_k[m+i]c_J^*[m]\right.\\ \qquad\left.+\sum\limits_{m=(n+1)\mathrm{SF}-i-1}^{(n+1)\mathrm{SF}-1}\frac{\tau'}{T_c}c_O[m+i+1]c_O[m]c_k[m+i+1]c_J^*[m]\right\}, & \tau<0\end{cases} \tag{A9}$$

$$\gamma_{k,p;J,f}^{\prime(n)}(\tau)=\begin{cases}\frac{1}{2\mathrm{SF}}\left\{\sum\limits_{m=n\mathrm{SF}+i}^{(n+1)\mathrm{SF}-1}\frac{T_c-\tau'}{T_c}c_O[m]c_k[m-i]c_J^*[m]+\sum\limits_{m=n\mathrm{SF}+i+1}^{(n+1)\mathrm{SF}-1}\frac{\tau'}{T_c}c_O[m]c_k[m-i-1]c_J^*[m]\right\}, & \tau\geq 0\\ \frac{1}{2\mathrm{SF}}\left\{\sum\limits_{m=n\mathrm{SF}}^{(n+1)\mathrm{SF}-i-1}\frac{T_c-\tau'}{T_c}c_O[m]c_k[m+i]c_J^*[m]+\sum\limits_{m=n\mathrm{SF}}^{(n+1)\mathrm{SF}-i-2}\frac{\tau'}{T_c}c_O[m]c_k[m+i+1]c_J^*[m]\right\}, & \tau<0\end{cases} \tag{A10}$$

and

$$\dot{\gamma}_{k,p;J,f}^{\prime(n)}(\tau)=\begin{cases}\frac{1}{2\mathrm{SF}}\left\{\sum\limits_{m=n\mathrm{SF}}^{n\mathrm{SF}+i-1}\frac{T_c-\tau'}{T_c}c_O[m]c_k[m-i]c_J^*[m]+\sum\limits_{m=n\mathrm{SF}}^{n\mathrm{SF}+i}\frac{\tau'}{T_c}c_O[m]c_k[m-i-1]c_J^*[m]\right\}, & \tau\geq 0\\ \frac{1}{2\mathrm{SF}}\left\{\sum\limits_{m=(n+1)\mathrm{SF}-i}^{(n+1)\mathrm{SF}-1}\frac{T_c-\tau'}{T_c}c_O[m]c_k[m+i]c_J^*[m]+\sum\limits_{m=(n+1)\mathrm{SF}-i-1}^{(n+1)\,rmSF-1}\frac{\tau'}{T_c}c_O[m]c_k[m+i+1]c_J^*[m]\right\}, & \tau<0\end{cases} \tag{A11}$$

We rearrange the above results and obtain (A4) and (A5), shown at the bottom of the previous page. In addition, we have (A6)–(A11), shown at the top of the page.

REFERENCES

[1] J. G. Proakis, *Digital Communications*, 4th ed. New York: McGraw-Hill, 2000.

[2] S. Verdú, *Multiuser Detection*. Cambridge, U.K.: Cambridge Univ. Press, 1998.

[3] S. Verdú, "Minimum probability of error for asynchronous Gaussian multiple-access channels," *IEEE Trans. Inf. Theory*, vol. IT-32, no. 1, pp. 85–96, Jan. 1986.

[4] A. J. Viterbi, "Very low rate convolution codes for maximum theoretical performance of spread-spectrum multiple-access channels," *IEEE J. Sel. Areas Commun.*, vol. 8, no. 4, pp. 641–649, May 1990.

[5] M. K. Varanasi and B. Aazhang, "Multistage detection in asynchronous code-division multiple-access communications," *IEEE Trans. Commun.*, vol. 38, no. 4, pp. 509–519, Apr. 1990.

[6] D. Divsalar, M. K. Simon, and D. Raphaeli, "Improved parallel interference cancellation for CDMA," *IEEE Trans. Commun.*, vol. 46, no. 2, pp. 258–268, Feb. 1998.

[7] P. Patel and J. Holtzman, "Analysis of a simple successive interference cancellation scheme in a DS/CDMA system," *IEEE J. Sel. Areas Commun.*, vol. 12, no. 5, pp. 796–807, Jun. 1994.

[8] M. Juntti and B. Aazhang, "Finite memory-length linear multiuser detection for asynchronous CDMA communications," *IEEE Trans. Commun.*, vol. 45, no. 5, pp. 611–622, May 1997.

[9] P. R. Patel and J. M. Holtzman, "Performance comparison of a DS/CDMA system using a successive interference cancellation (IC) scheme and a parallel IC scheme under fading," in *Proc. IEEE ICC*, 1994, vol. 1, pp. 510–514.
[10] A. Duel-Hallen, J. Holtzman, and Z. Zvonar, "Multiuser detection for CDMA systems," *IEEE Pers. Commun.*, vol. 2, no. 2, pp. 46–58, Apr. 1995.
[11] J. Hou, J. E. Smee, H. D. Pfister, and S. Tomasin, "Implementing interference cancellation to increase the EV-DO Rev a reverse link capacity," *IEEE Commun. Mag.*, vol. 44, no. 2, pp. 96–102, Feb. 2006.
[12] J. G. Andrews and T. H. Meng, "Optimum power control for successive interference cancellation with imperfect channel estimation," *IEEE Trans. Wireless Commun.*, vol. 2, no. 2, pp. 375–383, Mar. 2003.
[13] D.-K. Hong, Y.-H. You, S.-S. Jeong, and C.-E. Kang, "Pipelined successive interference cancellation scheme for a DS/CDMA system," in *Proc. IEEE WCNC*, 1999, vol. 3, pp. 1489–1492.
[14] C.-H. Tang and C.-H. Wei, "Pilot-channel aided pipeline scheme for interference cancellation in uplink DS/CDMA system," in *Proc. IEEE 56th VTC—Fall*, Sep. 24–28, 2002, vol. 4, pp. 2361–2365.
[15] R. M. Buehrer, "Equal BER performance in linear successive interference cancellation for CDMA systems," *IEEE Trans. Commun.*, vol. 49, no. 7, pp. 1250–1258, Jul. 2001.
[16] J. H. Kim and S. W. Kim, "Combined power control and successive interference cancellation in DS/CDMA communications," in *Proc. 5th Int. Symp. Wireless Pers. Multimedia Commun.*, 2002, vol. 3, pp. 931–935.
[17] J. G. Andrews and T. H. Meng, "Transmit power and other-cell interference reduction via successive interference cancellation with imperfect channel estimation," in *Proc. IEEE ICC*, 2001, vol. 6, pp. 1940–1944.
[18] P. Hatrack and J. M. Holtzman, "Reduction of other-cell interference with integrated interference cancellation/power control," in *Proc. IEEE 47th Veh. Technol. Conf.*, May 1997, vol. 3, pp. 1842–1846.
[19] D. Warrier and U. Madhow, "On the capacity of cellular CDMA with successive decoding and controlled power disparities," in *Proc. IEEE 48th VTC*, May 1998, vol. 3, pp. 1873–1877.
[20] C. C. Chan and S. V. Hanly, "The capacity improvement of an integrated successive decoding and power control scheme," in *Proc. IEEE 6th Int. Conf. Universal Pers. Commun.*, Oct. 1997, vol. 2, pp. 800–804.
[21] R. M. Buehrer and R. Mahajan, "On the usefulness of outer-loop power control with successive interference cancellation," *IEEE Trans. Commun.*, vol. 51, no. 12, pp. 2091–2102, Dec. 2003.
[22] J. G. Andrews, A. Agrawal, and T. H. Meng, "Iterative power control for imperfect successive interference cancellation," *IEEE Trans. Wireless Commun.*, vol. 4, no. 3, pp. 878–884, May 2005.
[23] 3GPP Technical Specification Group RAN, *Spreading and Modulation (FDD) (Release 5)*, 3GPP, TS 25.213, 2002.
[24] R. Fantacci and A. Galligani, "An efficient RAKE receiver architecture with pilot signal cancellation for downlink communications in DS-CDMA indoor wireless networks," *IEEE Trans. Commun.*, vol. 47, no. 6, pp. 823–827, Jun. 1999.
[25] D.-K. Hong, T.-Y. Kim, D. Hong, and C.-E. Kan, "Pilot to data channel power allocation for PCA-DS/CDMA with interference canceler," *IEEE Commun. Lett.*, vol. 5, no. 8, pp. 331–333, Aug. 2001.
[26] C.-H. Tang, W.-Y. Chang, and C.-H. Wei, "Pilot channel aided adaptable interference cancellation scheme for uplink DS/CDMA mobile radio systems," in *Proc. IEEE GLOBECOM*, Nov. 25–29, 2001, vol. 5, pp. 3163–3167.
[27] M. Ewerbring, B. Gudmundson, P. Teder, and P. Willars, "CDMA-IC: A proposal for future high capacity digital cellular systems," in *Proc. IEEE 43rd VTC*, May 18–20, 1993, pp. 440–443.
[28] P. R. Patel and J. M. Holtzman, "Analysis of a DS/CDMA successive interference cancellation scheme using correlations," in *Proc. IEEE Conf. Global Telecommun.*, Houston, TX, 1993, vol. 1, pp. 76–80.
[29] R. M. Buehrer, S. P. Nicoloso, and S. Gollamudi, "Linear versus non-linear interference cancellation," *J. Commun. Netw.*, vol. 1, no. 2, pp. 118–133, Jun. 1999.
[30] K. Puttegowda, G. Verma, S. Bali, and R. M. Buehrer, "On the effect of cancellation order in successive interference cancellation for CDMA systems," in *Proc. IEEE 57th Conf. Veh. Technol.—Fall*, Orlando, FL, Oct. 2003, vol. 2, pp. 1035–1039.
[31] C.-H. Tang and C.-H. Wei, "Pilot-channel aided successive interference cancellation for uplink WCDMA systems over multipath fading channels," in *Proc. IEEE Int. Symp. Commun. Inf. Technol.*, Oct. 2004, pp. 149–153.
[32] J. Weng, G. Xue, T. Le-Ngoc, and S. Tahar, "Multistage interference cancellation with diversity reception for asynchronous QPSK DS/CDMA systems over multipath fading channels," *IEEE J. Sel. Areas Commun.*, vol. 17, no. 12, pp. 2162–2180, Dec. 1999.
[33] Y. C Yoon, R. Kohno, and H. Imai, "A spread-spectrum multiaccess system with cochannel interference cancellation for multipath fading channels," *IEEE J. Sel. Areas Commun.*, vol. 11, no. 7, pp. 1067–1075, Sep. 1993.
[34] A. C. K. Soong and W. A. Krzymien, "A novel CDMA multiuser interference cancellation receiver with reference symbol aided estimation of channel parameters," *IEEE J. Sel. Areas Commun.*, vol. 14, no. 8, pp. 1536–1547, Oct. 1996.
[35] H. A. David, *Order Statistics*. New York: Wiley, 1981.
[36] 3GPP Technical Specification Group RAN, *BS Radio Transmission and Reception (FDD) (Release 5)*, 3GPP, TS 25.104, 2002.
[37] L. K. Rasmussen, S. Sumei, T. J. Lim, and H. Sugimoto, "Impact of estimation errors on multiuser detection in CDMA," in *Proc. IEEE 48th VTC*, May 1998, vol. 3, pp. 1844–1848.
[38] C.-H. Tang and C.-H. Wei, "Pilot-channel aided SIC scheme for multirate WCDMA systems in multipath fading channels," in *Proc. IEEE 62nd VTC—Fall*, Sep. 25–28, 2005, vol. 3, pp. 1980–1983.

Chih-Hsuan Tang (S'01) received the B.S. degree in electronics engineering from National Chiao Tung University (NCTU), Hsinchu, Taiwan, R.O.C., in 1997 and the Ph.D. degree from the Institute of Electronics, NCTU, in 2007.

Her research interests are in the area of wireless communications, multiuser detection, and iterative decoding.

Che-Ho Wei (S'73–M'76–SM'87–F'96) received the B.S. and M.S. degrees in electronics engineering from National Chiao Tung University (NCTU), Hsinchu, Taiwan, R.O.C., in 1968 and 1978, respectively, and the Ph.D. degree in electrical engineering from the University of Washington, Seattle, in 1976.

From 1976 to 1979, he was an Associate Professor at National Chiao Tung University. From 1979 to 1982, he was an Engineering Manager at Wang Industrial Company, Taipei, Taiwan. From 1982 to 1986, he served as the Chairman in the Department of Electronics Engineering, NCTU, and from 1984 to 1989, as Director in the Institute of Electronics, NCTU. From September 1990 to July 1992, he was on leave at the Ministry of Education and served as the Director at the Advisory Office. From August 1993 to July 1995, he was Dean of Research of NCTU, from August 1995 to July 1998, was Dean of the College of Electrical Engineering and Computer Science, and from November 1998 to March 2001, was Vice President. From March 2001 to May 2004, he was appointed as the Chairman of the National Science Council of R.O.C. He is currently a Professor Emeritus at NCTU. His research interests include digital communications and signal processing and related circuit design.

Dr. Wei was the founding Chairman of Taipei Chapter of IEEE Circuits and Systems Society and IEEE Communication Society. From 1992 to 1994, he served as a member of the Board of Governors, IEEE Circuits and Systems Society. From 1990 to 1996, he was the recipient of the Distinguished Research Award from the National Science Council of R.O.C. He was elected as an IEEE Fellow in 1996 for his contributions to circuits and systems for communications and signal processing. He was the recipient of the Academic Achievement Award from the Ministry of Education of R.O.C. in 2000. He was the recipient of the IEEE Third Millennium Medal and IEEE Circuits and Systems Society Golden Jubilee Medal in 2000.